Journal of Geoscience and Environment Protection, 2022, 10, 126-160
https://www.scirp.org/journal/gep
ISSN Online: 2327-4344
ISSN Print: 2327-4336

Effects of Increasing Impervious Surface on Water Quality in Ile-Ife Urban Watershed, Southwestern Nigeria

Olusola-Ige Olufayo Adetoro[1*], Victor Osarenren[1], Samuel Oladimeji Popoola[1,2]

[1]Space Applications and Environmental Science Laboratory, Institute of Ecology and Environmental Studie, OAU, Nigeria Obafemi Awolowo University, Ile-Ife, Nigeria
[2]Information Network, Regional Advanced Space Technology Application Laboratory, National Space Research and Development Agency (NASRDA), Ile-Ife, Nigeria
Email: *omoige@gmail.com

How to cite this paper: Adetoro, O.-I. O., Osarenren, V., & Popoola, S. O. (2022). Effects of Increasing Impervious Surface on Water Quality in Ile-Ife Urban Watershed, Southwestern Nigeria. *Journal of Geoscience and Environment Protection, 10,* 126-160.
https://doi.org/10.4236/gep.2022.1012010

Received: November 15, 2022
Accepted: December 25, 2022
Published: December 28, 2022

Abstract

The urban environment has continued to experience changes from increasing impervious surfaces, which alters the proper functioning of the ecological zones and impairs water quality in the watershed. Impervious cover is predominantly used as an indicator to assist in understanding and forecasting the impact of human actions and other related activities on aquatic resources. In this study, the rate of change in land uses using the impervious surface as an indicator, and the percentage of imperviousness on the effect on water quality in the urban watershed were assessed. Ile-Ife was delineated as an urban watershed, and the percentage of imperviousness from 2008 to 2016 and the effect of imperviousness on water bodies were assessed. The study utilized ASTERDEM, Worldview (0.46 m), IKONOS (1.4 m), Landsat (30 m) for 2008 and 2016, GPS and Drone (10 cm). Water sampling was carried out in selected locations as generated by the impervious surface analyst tool, (ISAT). The percentage (%) of impervious surfaces accounted for 59.4% (4567.1/7691.5ha) in 2008 and 70.3% (5408.2/7691.5ha) in 2016, from the total number of lands investigated. The turbidity values from low to high regions were 32.3, 55.9 and 82.4 NUT. Changes in LULC of the watershed led to increased surface temperature, impermeable surfaces, and decreased vegetation, which exposes the area to flooding and reduced water quality. This study emphasized the importance of GIS and its integration into urban changes and water quality assessment.

Keywords

Urban Watershed, Impervious Surface, Water Quality, ISAT, OBIA,

Turbidity

1. Introduction

Globally, the urban environment has continued to experience land cover changes with the exchange of vegetation and water to impervious surfaces (Hua et al., 2020) and thereby increasing vegetation loss and highly impaired water bodies (Kaufmann et al., 2007; Xu et al., 2012; Ige-Olumide & Salami, 2018). The developing regions of the world most especially are extensively experiencing urbanization and each of its major regions will hold more cities than rural dwellers by the year 2030 as projected by the United Nations (UN) Population Division. It is also estimated that by 2050, two-thirds of the inhabitants in developing countries are probably going to live in metropolitan areas (Montgomery, 2008). Wu (2014) and United Nations (2013) emphasized that there has been a phenomenal population expansion in urban communities around the world (Farrell, 2017; Ritchie & Roser, 2018; Kuddus et al., 2020; Hua et al., 2020) which has prompted urban landscape changes. The population changes due to urbanization are increasing massively in developing regions and this exerts pressure on natural resources (Wang et al., 2018; Wang et al., 2020). This leads to the loss of forests, productive agricultural land, shrinking/loss of surface water bodies, other green open spaces, and perhaps irreversible damage to the earth's ecological and environmental systems (Couch et al., 2005; Elmqvist et al., 2016).

Changes in these land use forms or initial cover are identified as some of the effects of urbanization (Mugiraneza et al., 2019a; Fernández-Götz et al., 2014). The erection of high-rise buildings, and the conversion of towns to urban areas and megacities are presently in operation, especially where there is a sporadic population increase. Urbanization has led to several ecological challenges which transcend from small to large scale (Zhao et al., 2006), incorporating various pollution types and reduced water availability (Shao et al., 2006), increased energy demands and nearby atmosphere modification (Zhou et al., 2004; González et al., 2005), inadequate infrastructures in urban areas (Jago-on et al., 2009), and a substantial loss of forest resources and carbon stock (Fang et al., 2003; Yuan, 2008). Increased urban growth causing negative changes to the ecological environment affects the quality of life which is most evident in the developing world without adaptative mechanisms (Rahman et al., 2011). United Nations (UN) (2013) established that the Sub-Saharan population increase will be roughly from 769 million to about 1.69 billion which is attributed to urban sprawl occurring in small and big cities. Given these projections, it is proposed that urban communities in developing nations should build impenetrable surface regions to sustain the present population expansion (United Nations (UN) (2013). Urban areas are becoming precipitous around the world, and the effect of urbanization will always bring along with it global, regional and local changes consistently. Urban expansion cannot be overlooked in LULC research (Rana, 2011). Developing countries are experiencing an unprecedented increase in population and urban expansion (United Nations (UN), 2013), which increases the percentage of impervious surfaces and probably elongates the severity of its impact on the copying capacity of the world (Raddad et al., 2010).

Impervious surface (IS) which is described as an urban area indicator from history is presently regarded as an environmental factor (Xu et al., 2012; Gillies et al., 2003; Arnold & Gibbons, 1996) used to address the various framework of complex environmental issues and predominately in urban and semi-urban areas. This ranges from its impact on water quality (Brabec et al., 2002; Arnold & Gibbons, 1996; Fu et al., 2019), rainfall run-off (Lohani et al., 2002; Aladejana, 2021; Brun & Band, 2000), and the urban heat island effect (Weng et al., 2004; Chen et al., 2006; Yuan & Bauer, 2007; Ige-Olumide & Garuba, 2018). Many land use planners and water resource stakeholders face extreme challenges of uncontrolled urban growth/sprawl and sometimes unmanaged construction development and their deleterious impacts on water quality (Kauffman & Brant, 2000). They emphasized that watershed impervious cover threshold or hotspot can be utilized to address growth into watershed zoning districts by identifying locations where the least impact on stream water quality will be recorded due to development. As the imperviousness of a watershed increases, the greater volume of stormwater increases the possibility of flooding (Fabiyi, 2006; Adetoro & Salami, 2018; Aderogba, 2012; Weng & Lu, 2008) and reduces the potential for pollutants to settle out; meaning that more pollution is delivered to drinking water streams and aquifers (Zhang, 2012). Too much paving and hardening of a watershed can reduce infiltration and groundwater levels which in turn can decrease the availability of aquifers, streams and rivers for drinking water supplies.

Over the years, impenetrable surfaces are being used as one of the key indicators for city climate transformation (Yuan & Bauer, 2007; Morabito et al., 2018; Ige-Olumide & Garuba, 2018). Impervious surface is recognized as a key factor in the growth, monitoring and strategic planning of the watershed because of the effect on the health of the ecosystem (Arnold & Gibbons, 1996; Wu, 2009; Sugg et al., 2014). The advent of urban sprawl has resulted in the increase and number of impenetrable surfaces such as concretes, asphalts, etc. and a decrease in the extent of vegetated lands, wetlands, and other forms of open space that ingest and clean stormwater within a natural framework. Impervious surface (IS) coverage can be selected as a key and quantifiable factor/indicator of water quality (Kauffman & Brant, 2000). Increasing amounts of impervious cover contribute significantly to too many of the water quality and quantity issues facing cities today (Flinker, 2010; Wu, 2013; Wang et al., 2018). These surfaces prevent water from infiltrating into the ground and creating stormwater runoff (Millennium Ecosystem Assessment (M.E.A.), 2005; Raudsepp-Hearne et al., 2011). This runoff then carries organic matter, fertilizers, pesticides, oil and grease and other contaminants, directly into streams, water bodies, and local water supplies. Additionally, because water runs quickly off these surfaces, the quantity and velocity of runoff are increased, the physical structure of streams becomes altered and eroded, and there is a greater likelihood of more frequent and larger floods time (Daramola & Ibem, 2010; Wang et al., 2018; Aderogba, 2012). The degree of damage to watershed health depends on many factors: the nature of existing land uses or the topography, soils, and vegetation (Furniss et al., 2010; Ahn & Kim, 2017). For this reason, it can be difficult to attribute environmental impairment to just one source and therefore often hard to prevent or predict (Hassan & Lee, 2015). However, impervious cover, while perhaps not always the direct cause of environmental impairments, is a good representative substitute.

Numerous studies have demonstrated a correlation between impervious cover levels and the environmental integrity of streams, and their watersheds and this correlation can then be used to predict and manage both water quality and watershed health (Xian & Crane, 2006; Weng & Lu, 2008; Jacobson, 2011; Liu et al., 2012). Therefore, it is crucial to understand the specific percentage of IS extent linked with various urban and suburban land uses/cover. The main concerns in this study are those attributed to the health of water resources. The rate of change in the impervious surface in a settlement can be a reflector of the composition of the landscape (biotic, hydrologic and geomorphic) of the area (Paul & Meyer, 2001). The magnitude, location and spatial pattern of impervious surfaces induce many physical and biological changes affecting the urban watershed.

Geographic information science and remote sensing display higher data source potential adopted for the extraction of IS from global to local scales (Cai et al., 2016). Medium spatial resolution images such as Landsat, Enhanced Thematic Mapper Plus (ETM+) images, Operational Land Imager (OLI), Satellite Pour l'Observation de la Terre (SPOT), and China-Brazil Earth Resources Satellite (CBERS) images and ASTER images have been utilized globally in IM extraction (Yang et al., 2003; Pu et al., 2008; Powell et al., 2007; Zhang et al., 2009; Luo & Mountrakis, 2010; Lu et al., 2011; Zhang et al., 2014; Parece & Campbell, 2013; Cai et al., 2016). Low to medium resolution is considered very coarse for visible extraction analysis because of the heterogeneity in the urban landscape and the complexity of urban IS materials (Jensen & Cowen, 1999; Lu & Weng, 2004; Zhang et al., 2014). Due to challenges such as low accuracy (Wu & Murray, 2003; Lu & Weng, 2006) attributed to the mixed pixel classification due to low spatial resolution and the heterogeneity of urban features (Cai et al., 2016), spectral mixture analysis has been widely adopted for deriving IS. In recent times, high resolution (HR) images where mixed pixels are highly reduced such as those from WorldView-2 Ikonos, and GeoEye-1 satellites, adopted in the derivation IS have revealed more reliable results (Cai et al., 2016; Li et al., 2011). Various techniques are considered for the extraction of the impervious surface using very high-resolution images. Very high-resolution images, which include sub-pixel analysis (Ji & Jensen, 1999; Lu & Weng, 2009; Sun et al., 2020), the pixel-based method (Wu & Murray, 2003; Lu et al., 2011; Xu & Tang, 2013; Wei & Blaschke, 2018), the object-based method (Blaschke, 2010; Hu & Weng, 2011; Liu et al., 2020) and the pixel- and object-based hybrid method (Li et al., 2013; Zhang et al., 2014; Wei & Blaschke, 2018). Many studies have demonstrated the capability of object-based techniques to produce a better result than the pixel-based method or sub-pixel analysis (Blaschke, 2010; Lu et al., 2011; Wei & Blaschke, 2018). The object-based method in recent times is recognized to be effective for IS mapping from very high-resolution images (VHR) (Zhou & Troy, 2008; Blaschke, 2010; Wei & Blaschke, 2018). However, other problems are identified in IS derivation using very high resolution images. Most of this involves spectral challenges between IS and other classes. The reason for this is attributed to the low spectral resolution of very high resolution images and the high spectral variation of impervious surfaces; noise (shadows) from high objects, such as built ups and natural canopies (Hu & Weng, 2011). More classification of the grey portion is mostly considered as an option in other works to resolve this problem (Blaschke, 2010; Li et al., 2011; Wei & Blaschke, 2018; Liu et al., 2020). The recent use of Unmanned aerial vehicles/systems (UAV/S) to provide aerial images to support ground-truthing for accuracy assessment is of recent use (Feng et al., 2015; Popoola et al., 2016; Kalantar et al., 2017; Yao et al., 2019) to address some of these identified challenges and improve accuracy.

Adequate clarity on impervious surface changes is key to various ecological applications, for example, assessment of the impact of a watershed (Jennings & Jamagin, 2002), precipitation runoff volume, intensity, and length (Lohani et al., 2002), groundwater revive and base flow storm analysis, storm flow and flood recurrence (Brun & Band, 2000). Thus, producing a timely and accurate impervious surface distribution map is crucial to various challenges and matters related to worldwide ecological change. The overall objective of this study was to OBIA for the extraction of impervious surfaces from two VHR images of different years in an urban watershed and to investigate the effect of impervious surfaces on water quality using integrated data in the impervious surface analyst tool (ISAT).

2. Materials and Methods

2.1. Study Area

The study area is the urban settlement of Ile-Ife which is an ancient Yoruba town in southwestern Nigeria. The city lies between Latitudes 7˚28'N and 7˚45'N and Longitudes 4˚30'E and 4˚34'E as described in **Figure 1**. The city is located right at the center of the Yoruba-speaking states in West Africa and about 200 km NE of Lagos, which is Nigeria's coastal capital city for over a century (Olupona, 2011). The rate of urbanization of Ile-Ife is dated back to approximately 500 ADS (Mabogunje, 1968, 1980) and has a social-cultural group known as the Yoruba ethnic group (one of the largest ethnic groups in Africa) (Levinson, 1998; Olupona, 2011). It is one of the popular towns of Osun state, extending over parts of Ife Central, East and North Local Government areas with a population of 644,373 (NPC, 2015).

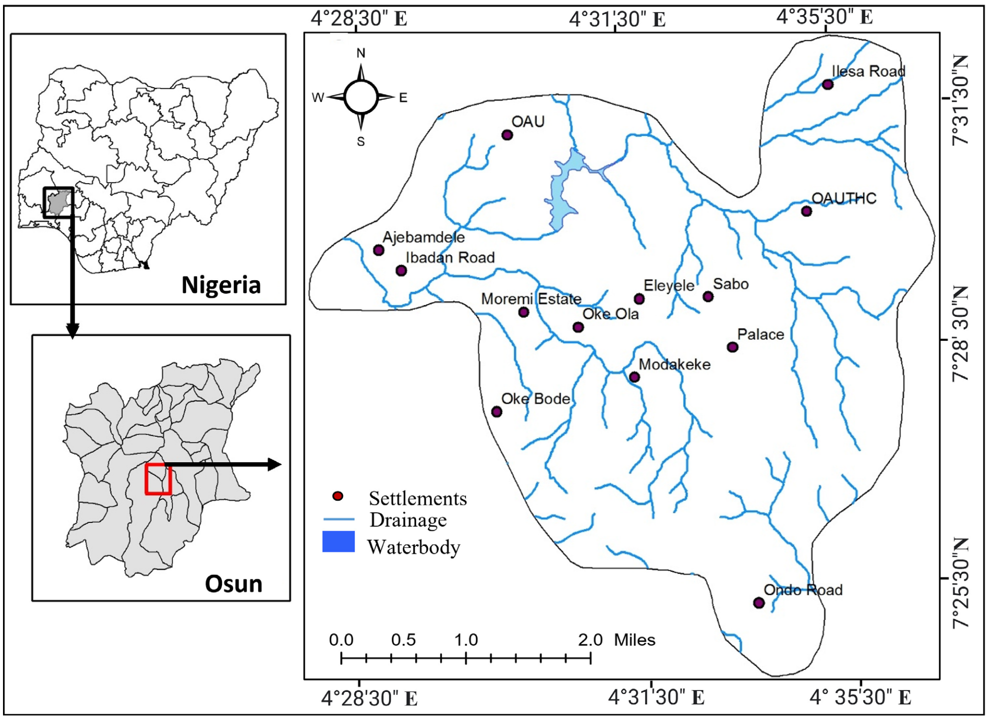

Figure 1. Urban Area of Ile-Ife, Southwestern Nigeria, West Africa.

2.2. Data Sources and Sample Collection

To delineate the urban area into the watershed, the Advanced Spaceborne Thermal Emission and Reflection and Radiometer (ASTER) Global Digital Elevation Model (DEM) of 30 m spatial resolution from the archive of the U.S National Aeronautics and Space Administration (NASA). This is important for geospatial assessment and applications for catchment delineation, flood risk assessment, and the estimation of the transfer of pollutants and essential nutrients (Gaafar et al., 2020; Giannoni et al., 2005). The WorldView-2 image was acquired from the Digital Globe Foundation archive. The WorldView-2 sensor provides a high-resolution panchromatic band and eight multispectral bands (Nouri et al., 2014; Park et al., 2020): four standard colors (red, green, blue, and near-infrared 1) and four new bands (coastal, yellow, red edge, and near-infrared 2). The worldview provides 0.46 m panchromatic mono and stereo satellite image data (Nouri et al., 2014). The IKONOS image was also acquired from the archive of Space Application and Environmental Science Laboratory, Obafemi Awolowo University. It's a commercial Earth observation satellite at 1 - 4-meter resolution (Fraser et al., 2002) that collects multispectral and panchromatic imagery. The population density was extracted from the ward map featuring the three local governments that fall within the watershed under study namely, Ife Central local government, Ife East local government and Ife North local government. **Table 1** provides a summary of the data used and the relevance for the study.

2.3. Field Survey and Accuracy Assessment

Ground truthing and field surveys using GPS receiver and recently archived

UAV aerial images were utilized to facilitate more accurate interpretation of the satellite imageries, identify and verify important areas and other features as well as the classification accuracy assessment points on the ground and other salient features. Several points of interest were identified on the topographic map for easy navigation and identification of the area of interest on the ground. Areas of interest were identified on the field and their spatial and attribute information was recorded with a GPS and a field note. Most areas of interest on the map were accessible and this provided a better visual understanding and interpretation of the images during classification. After satisfactory visual interpretation of the images, the following land use and land cover types were identified and the layers created: Built-ups, roads, vegetation and water body. The Built-up comprises buildings and artificial structures. The vegetation represents areas covered by trees of different species and sizes, shrubs and woody plants, etc. water body refers to ground surface water. The visual interpretation was done employing the interpretation keys such as size, shape, texture, pattern, tone, color and association of features. Accuracy Assessment as reflected in most existing studies that used very high resolution (VHR) images for impervious surface extraction (e.g., Lu & Weng, 2009; Lu et al., 2011; Zhang et al., 2014; Sugg et al., 2014), reference data for both training and validation were mainly collected by visual interpretation of aerial photography acquired by low altitude UAV (unmanned aerial vehicle), VHR WorldView-2 images, and IKONOS images. Those samples of which the attributes are difficult to determine on remotely sensed data (e.g., the samples in shaded areas) were checked from the ground survey and acquired UAV aerial image. A ground survey was subjected to a probability sampling protocol involving stratified random sampling (Henrys & Jarvis, 2019) which was used to identify the locations at which validation points were obtained. This sampling method has been used widely and shown to improve sampling efficiency by reducing inconsistency within a stratum and increasing variability between strata (Jin et al., 2014).

2.4. Methodological Approach

Table 1. Datasets, characteristics, sources and relevance to the study.

Data	Characteristics	Source	Relevance
DEM	30 m	USGS	Delineate urban watershed (basin map) and generation of elevation data and slope.
High-resolution satellite images	Worldview-2 2016 (0.46 m) and IKONOS 2008 (1.4 m)	Digital Globe Foundation and Space Application and Environmental Laboratory, Obafemi Awolowo University.	Dynamics in the type of LULC with object-based image analysis (OBIA)
Medium resolution satellite image	Landsat MSS, TM, ETM$^+$ and OLI (path 190, 191 and row 55). 2008, 2016.	Global land cover Facility (GLCF)	Derived Land Surface Parameters which are Land Surface Temperature, NDVI, Emissivity, and Brightness Temperature.

Continued

Impervious Surface Analysis Tool (ISAT).	Hydrological unit, Land Cover Grid, Impervious Surface Coefficient and Population data.	The National Oceanic and Atmospheric Administration (NOAA) Coastal Service Center.	Assess the correlation between the increase in impervious surface and decrease in water quality in small watersheds.
Location Data	Longitude and Latitude	GPS and UAV (Drone) of 10 cm	Assess more precise interpretations of the satellite imageries, Identify and validate significant areas and other features as well as the post classification points on the ground. Identify sampling points generated on the ISAT map

2.5. Urban Watershed Delineation

The urban watershed was delineated from the Digital Elevation Model (DEM) using ArcSWAT toolbox. The DEM was set to projected coordinate system using the Universal Transverse Mercator (UTM) projection with World Geodetic System (WGS) 1984 datum and zone 31N using ArcGIS 10.3. The DEM was supplied to the Automatic Watershed Delineator in ArcSWAT (Luo et al., 2011) with a mask of the extent of Landsat images of 190/55 and 191/55 combined. Flow direction and Flow accumulation were generated. Stream network and outlet creation followed. Outlet points were selected along the stream network to delineate the watershed (Lindsay et al., 2008; Tarboton, 1997). The fill dem was carried out to remove the depression from an elevation raster and a common method for removing a depression was applied which involves increasing the cell value to the lowest overflow point out of the sink (Jenson & Domingue, 1998). The flat surface resulting from sink filling was interpreted to define the drainage flow. This was achieved by imposing two shallow gradients and forcing flow away from higher terrain surroundings the flat surface towards the edge bordering lower terrain (Garbrecht & Martz, 1997). The flow direction raster was carried out. Flow direction raster was carried out using a single D8. The cells' flow direction was assigned to one of the eight surrounding cells that has the steepest distance-weighted gradient (O'Callaghan & Mark, 1984; Tarboton, 1997). The flow accumulation raster tabulates for each cell the number of cells that will flow to it. The tabulation is based on the flow direction raster. The flow accumulation raster records how many upstream cells will contribute drainage to each cell (Zhou et al., 2019).

2.6. Image Processing and Impervious Surface Extraction

This is an important phase in satellite image processing and analysis, which has an impact on all other subsequent procedures and results. The imageries were first pre-processed for geometric rectification. The image bands used for the study were geometrically rectified to the Geographic Coordinate System of the study area; WGS_84_UTM zone 31N. The shapefile of the study area was overlaid on the WorldView-2 satellite image and appropriate scenes of the image within the shapefile were selected. Each of the selected scenes was mosaicked to achieve a single image for further delineation. The shapefile of the study area was clipped from the mosaicked image (Blaschke et al., 2015) and gridlines were created over the scenes, numbering them into smaller scenes for easy use on the eCognition software.

2.6.1. Object-Oriented Classification

Image classification for the high-resolution satellite images was carried out on the eCognition developer software version 9.0. eCognition Developer is a development environment for object-based image analysis. It is used in earth science to develop rule sets (or applications) for the analysis of remote sensing data. The first step to image classification on eCognition was multiresolution segmentation. Image objects were extracted at modifiable scale parameters, single layer weights and the mixing of the homogeneity criterion concerning color and shape. The multi-Resolution segmentation (MRS) was adopted for this study which is a widely utilized algorithm embedded into ecognition (version 9.0, Trimble Germany GnbH, Munich, Germany, 2014). Bottom-up region (Fu et al., 2019; Blaschke, 2010) that uses a step wisely merges a small image into a larger image object until heterogeneity is reached. MRS was performed on the image using a scale parameter of 20, the domain was at the pixel level, while the composition of homogeneity criterion (Johnson & Xie, 2011) was applied also, with the shape at 0.1 and compactness at 0.5. This was done to ensure better segmentation thereby enhancing classification (Makinde et al., 2016; Russakovsky et al., 2015; Fu et al., 2019). The outcome of the segmentation is subject to several adjustable criteria—scale parameter, domain and homogeneity criterion (Blaschke, 2010; Fu et al., 2019). In particular, the scale parameter is a measure of the maximum change in heterogeneity that may occur when merging two image objects. A larger-scale parameter value leads to bigger objects and vice versa.

2.6.2. Arithmetic Feature

Arithmetic features are composed of existing features, variables, and constants, which are combined via arithmetic operations. Arithmetic features are composed of multiple features but apply only to a single object. After the multiresolution segmentation, an arithmetic feature was calculated, known as the *Greenness Index*. This is the ratio between the green band and the sum of the red band and the blue band.

$$\text{Greenness index} = \frac{\text{Meanlayer 2 (Green)}}{\text{Meanlayer 1} + \text{Meanlayer 3}}$$

According to the range of values gotten the boundary was 0.55, any object above 0.55 was vegetation and any object below 0.55 was not vegetation. The information derived from the greenness index aided in assigning classes. The features were assigned class names from the image object domain to a class array. The class was assigned based on the existing information, any object that has an arithmetic feature greater than 0.55 was classified as vegetation and any object that has an arithmetic feature lesser than 0.55 remained unclassified (Mugiraneza et al., 2019b; Makinde et al., 2016). This assisted in the separation of vegetation from other image objects. The shape index was used to determine the characteristics of other objects in the image. The Shape index describes the smoothness of an image object border. The smoother the border of an image object is, the lower its shape index (Lemenkova, 2015; Ikokou & Smit, 2013). From the value range of the shape index, objects greater than 3 were classified as roads and objects less than 3 belonged to other classes (Blaschke, 2010; Lemenkova, 2015). The relative border which describes the ratio of the shared border length of an image object (with a neighboring image object assigned to a defined class) to the total border length was also used (Flanders et al., 2003; Yang et al., 2019; Espriella et al., 2020). If the relative border of an image object to image objects of a certain class is 1, the image object is embedded in them. The relative border was calculated from the feature characteristics and objects with a relative border value of 1 were wrongly classified. The relative border was applied to misclassified objects to help recover them to the appropriate class. Furthermore, four classes were identified—Vegetation, Waterbody, Road, and Built-up. Two major classes (Impervious and Pervious) were further created from the classes above, with bare ground, roads and built up as Impervious and vegetation and water body as Pervious. All the feature objects in the same class were merged into a single multi-part polygon (impervious and pervious). The results were exported to a shapefile and opened on ArcGIS. On ArcGIS the study area (Ife urban shapefile) was clipped. Add geometry tool was used to calculate the total area of impervious cover and pervious covers in Square Meters which was eventually converted to Square Kilometers.

2.6.3. Percentage Imperviousness of the Urban Watershed

The percentage of the impervious surface area (PISA), which is defined as the ratio of impervious surface area to the total surface area of the watershed, has for many years been regarded as one of the useful indicators to measure the impacts of land development on the watershed environment.

$$\%\ \text{imperviousness} = \frac{\text{total value of impervious}}{\text{Total area}} * 100$$

2.6.4. Rate of Change in the Urban Watershed

The rate of change in the watershed between 2008-2016, was calculated using the formula;

$$\text{Rate of Change} = \frac{\text{recent year} - \text{later year}}{\text{year diference}}$$

$$\text{Rate of Change} = \frac{2016 - 2008}{8}$$

2.6.5. Effect of Imperviousness in the Urban Watershed

The effect of imperviousness in the watershed was studied for an important phenomenon in the environment which is Water Quality.

2.7. Impervious Surface Analyst Tool (ISAT)

The effect of imperviousness on water quality was determined using the Impervious Surface Analysis Tool (ISAT), which is available as a geographic information system script. It was used to calculate the percentage of impervious surface area within the study area. Information derived from ISAT was used to predict the different impacts on water quality. ISAT was developed by the National Oceanic and Atmospheric Administration (NOAA) Coastal Services, it is an American scientific agency within the United States Department of Commerce. The specific data utilized for the successful running of the ISAT tool includes Population Density Map; Land Cover Grid- land cover data; Hydrological Unit and Impervious Surface Coefficient

2.7.1. Population Density Map

The population density map was derived by getting the ward map from three local governments in the study area.

- Ife Central local government
- Ife East local government
- Ife North local government

These maps respectively were subjected to further geoprocessing.

The local government population values were resampled to the ward-level population using the number of buildings in each ward (simple relational association between building and population values). The number of buildings in each ward was related to the number of building in that same local government to derive the population for each ward, the population density was calculated by dividing by the area of each population value.

2.7.2. Water Quality Analysis

Water is a dynamic medium and its quality varies spatially and temporally. The change in the impervious-pervious stability has altered the stream water quality (Brabec et al., 2002; Kim et al., 2016). To accurately determine the effect of imperviousness on water quality it was important to carry out a water quality analysis in the study area (Burton & Pitt, 2002). Areas of sampling were carried out based on the result generated from the Impervious Surface Analyst Tool (ISAT). The parameters sampled were dissolved oxygen, biological oxygen demand, temperature, total dissolved solids, electrical conductivity and turbidity. The TDS meter, Model YL-TDS2-A which was first subjected to calibration (United States Environmental Protection Agency (USEPA), 2003; ISO, 2016) was used to test for total dissolved solids, electrical conductivity and temperature. The temperature measurement was carried out by using a portion of the water sample (1liter) and immersing the multi-parameter meter, Model YL-TDS2-A into it for a sufficient period until stabilization was reached (Kim et al., 2016) and reading was taken, expressed as ˚C. The electrical conductivity was achieved using the TDS meter, Model YL-TDS2-A which was dipped into the sample, and the readings were noted for the stable value shown as μs/cm.

Winkler's method was adopted for the measurement of dissolved oxygen (DO). DO bottles-300 ml capacity was used to collect the water sample. Manganous sulphate (2 ml) and 2 ml of potassium iodide were added and sealed. This is properly mixed and the precipitate was allowed to settle down. 2 ml of conc. Sulphuric acid was added and was adequately mixed until all the precipitate dissolved. Also, 203 ml of the sample is measured into the conical flask and titrated against 0.025N sodium thiosulphate using starch as an indicator. The endpoint is the change of color from blue to colorless. The biological oxygen demand was achieved by filling water samples into an airtight BOD bottle (Kim et al., 2016) and was incubated at room temperature for 5 days. The difference in the dissolved oxygen measured initially and after incubation gives the BOD of the sample. The total dissolved solid was derived by immersing the TDS meter into the sample for a sufficient period (till the reading stabilized) and the reading was taken and expressed as ppm (parts per million). Lastly for the sampling is the turbidity, which was determined using the instrumental method, the spectrophotometer at a wavelength of 430. The water samples were thoroughly shaken in the nephelometric tube and the values were recorded appropriately.

2.7.3. Hydrological Unit

The hydrological unit was derived from the delineation process carried out.

2.7.4. Land Cover Grid-Land Cover Data

The land use land cover map for the area was derived using a 2016 Planet Scope 3 meters multispectral satellite image in line with World view-2 image as recent images were required for accuracy purposes. The Planet scope image was classified using unsupervised classification, relating it to the Worldview image the following classes were identified: Built up, Vegetation, Waterbody, Road and Bare ground. This gave the land use land cover requirement for ISAT.

2.7.5. Impervious Surface Coefficients

The impervious coefficient was derived from the land use using the map algebra on ArcGIS. The impervious coefficient was determined based on the land use type as shown in **Table 2** below.

These values were generated based on the nature of the land use. The map algebra tool was used to calculate the value for each land use type. An excel spreadsheet was generated for the land cover impervious surface values and with the available parameters, the ISAT analysis was carried out.

3. Results

3.1. Delineated Watershed

The urban watershed of Ile-Ife in Osun state was delineated and the result is shown in **Figure 2** and **Table 3** which identifies the different catchments and places located within the urban watershed. The urban watershed was delineated

Table 2. Land use classes generated for impervious coefficient.

Land Use	Values
Wetlands	0
Built-up	100
Water	0
Bare surface	70
Forest	40
Shrubland	50
Grassland	60

Table 3. Delineated watershed in the urban watershed of Ile-Ife.

Watershed	Code Name	Area (ha)	Name of Settlements
A	WS_A	487.788	Ilesa Road
B	WS_B	226.812	Osu, Ibodi
C	WS_C	2223.252	Oke Bode, OAU, Adebamdele
D	WS_D	1504.430	Oke Ola, Modakeke, Moremi Estate
E	WS_E	142.641	Oke Otubu, Our lady's junction
F	WS_F	1093.871	Ondo Road
G	WS_G	2012.661	Eleyele, Sabo, Palace, OAUTHC.
		7691.5	

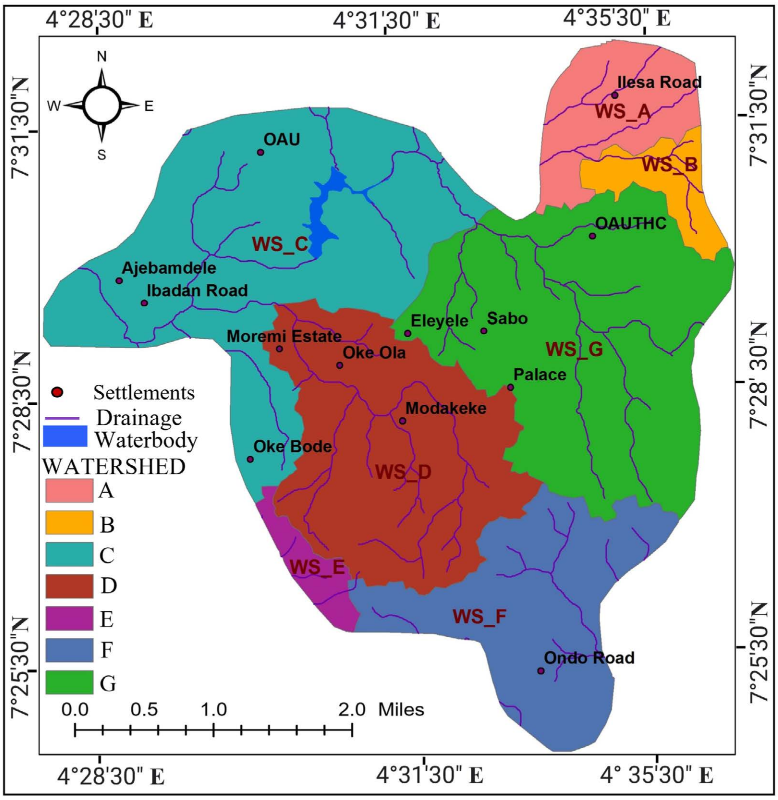

Figure 2. Watershed delineation of Ile-Ife Urban Watershed.

into 7 different watersheds, named alphabetically watersheds A to G. The area of each of the watersheds was determined and it was observed that watershed C was the largest watershed having an area of 2223.252 ha and the smallest watershed was E having an area of 142.641 ha. Other watersheds A, B, D, F and G covered an area of 487.788 ha, 226.812 ha, 1504.430 ha, 1093.871 ha and 2012.661 ha respectively, which makes watershed G the second largest in the study area. The urban watershed amounted to a total of 7691.455 ha.

3.2. Percentage Impervious Surface (%IS) of the Urban Watershed of Ile-Ife

The percentage of impervious surfaces in the watershed was analyzed using the object-oriented image classification and the result shows a drastic increase in an impervious layer over the years (2008-2016) in the respective watershed. Using object-oriented image classification (OBIA), the LULC was classified into four categories, which are; water, Built up, road and vegetation, which were classified with the seven urban watersheds that were delineated.

3.3. OBIA Classification for 2008 and 2016

The object image analysis classification for 2008 was obtained because of the classification carried out on each watershed. The study area was majorly made up of Built up, accounting for 4504.32 ha (59%), followed by vegetation 3076.65 ha (40%), water body 47.8 ha (0.8%) and road 62.8 (0.6%). The Total Area covered is 7691.5 ha (100%) as shown in **Figure 3**.

The object image analysis classification for 2016 was obtained because of the classification carried out on each watershed. The study area was mainly made up of Built up, accounting for 5334.9 ha (69%), followed by vegetation 2246.6 ha (29%), water body 36.72 ha (1%) and road 73.26 ha (1%). The Total Area covered is 7691.5 ha (100%) as shown in **Table 4** and **Figure 4**.

3.4. OBIA Re-Classification for 2008 and 2016

A reclassification was carried out for both 2008 and 2016 land features (**Table 5**, **Figure 4**). For 2008 Built up and roads were reclassified to the impervious surface, covering a surface area of 4567.1 ha (59.4%) while vegetation and water body were reclassified as pervious surface, covering a surface area of 3124.4 ha (40.6%). Built up and roads (impervious) for 2016 amounted to 5408.2 ha (70.3%) while vegetation and water body amounted to 2283.3 ha (29.7%) giving a total of 7691.5 ha (100%). The result showed an increase in impervious covers in 2016 as compared to 2008.

3.5. Rate of Change in the Watershed of Ile-Ife within the Years Studied

The change detection was determined in line with the result of the object-based image classification carried out on each watershed, and the classified maps of

Table 4. Land use land cover classification for each watershed.

Watershed	Year	Class names (%)				
		Built up (ha)	Vegetation (ha)	Road (ha)	Water (ha)	Total
A	2008	287.01 (59)	197.82 (41)	0.57 (0)	-	100
	2016	381.47 (78)	104.77 (22)	1.35 (0)	-	100
B	2008	117.45 (52)	104.67 (47)	1.44 (1)	-	100
	2016	189.69 (84)	34.98 (15)	2.61 (1)	-	100
C	2008	1111.41 (50)	1054.89 (47)	30.61 (1)	47.75 (2)	100
	2016	1623.18 (73)	528.21 (24)	37.53 (2)	36.72 (1)	100
D	2008	950.31 (63)	535.41 (36)	16.68 (1)	-	100
	2016	908.23 (60)	579.46 (39)	17.19 (1)	-	100
E	2008	85.68 (60)	56.97 (40)	-	-	100
	2016	109.47 (78)	32.55 (22)	-	-	100
F	2008	629.82 (58)	452.61 (41)	5.0 (1)	-	100
	2016	834.90 (76)	252.65 (23)	5.5 (1)	-	100
G	2008	1322.64 (66)	674.28 (34)	7.84 (1)	-	100
	2016	1289.94 (64)	713.985 (35)	11.25 (1)	-	100
TOTAL	2008	4504.32	3076.65	62.74	47.75	7691.5
	2016	5324.91	2246.6	73.26	36.72	7691.5

Table 5. Area covered for land use land cover in 2008 and 2016.

	Class Name	Area (ha)	Percentage (%)
2008	Built Up	4504.3	59.0
	Vegetation	3076.7	40.0
	Road	62.74	0.8
	Water	47.75	0.2
	Total	7691.5	100
2016	Built Up	5334.9	69.0
	Vegetation	2246.6	29.0
	Road	73.26	1.0
	Water	36.72	1.0
	Total	7691.5	100
Reclassified Land Use Land Cover for 2008 and 2016			
2008	Impervious	4567.1	59.4
	Non-Impervious	3124.4	40.6
	Total	7691.5	100
2016	Impervious	5408.2	70.3
	Non-Impervious	2283.3	29.7
	Total	7691.5	100

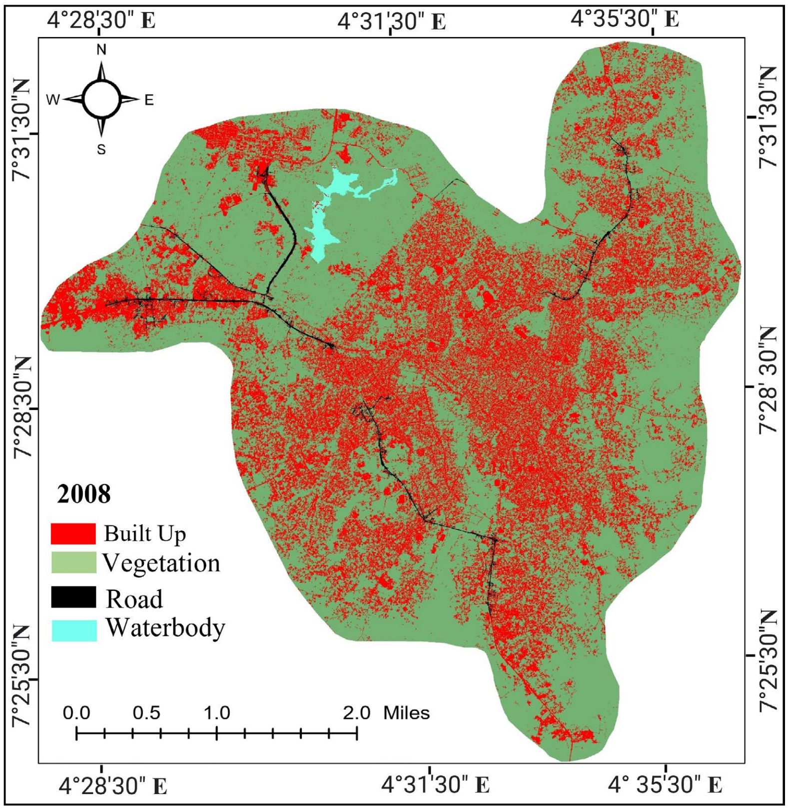

(A)

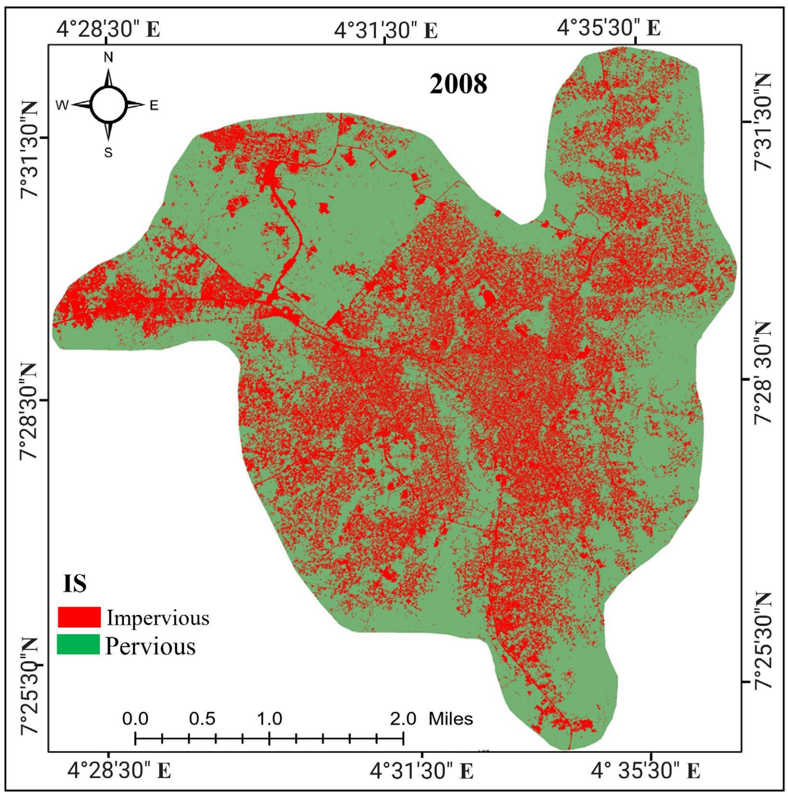

(B)

Figure 3. Classified object-based images for 2008 and 2016.

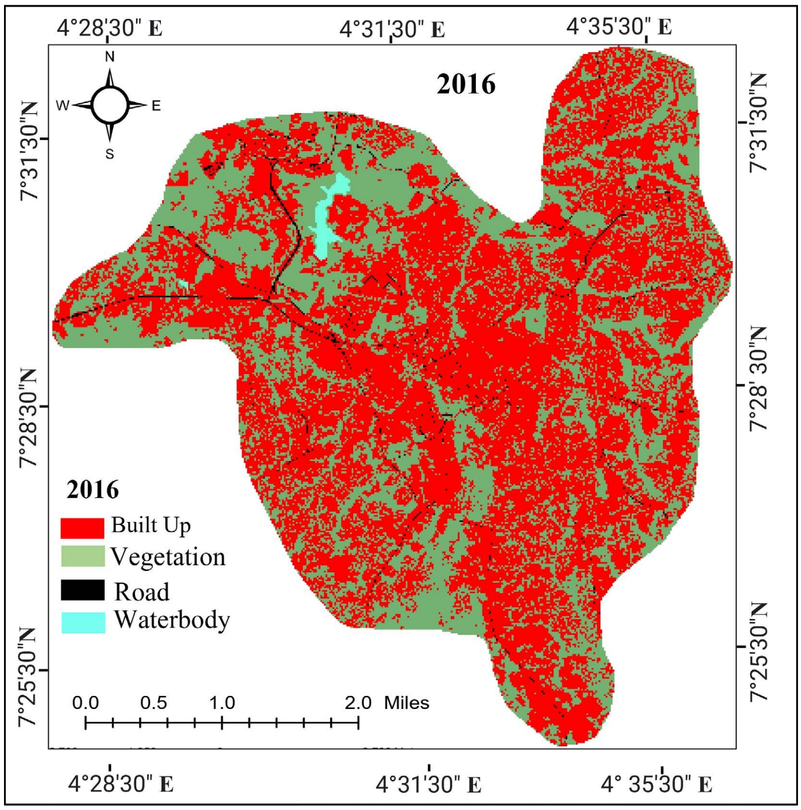

(A)

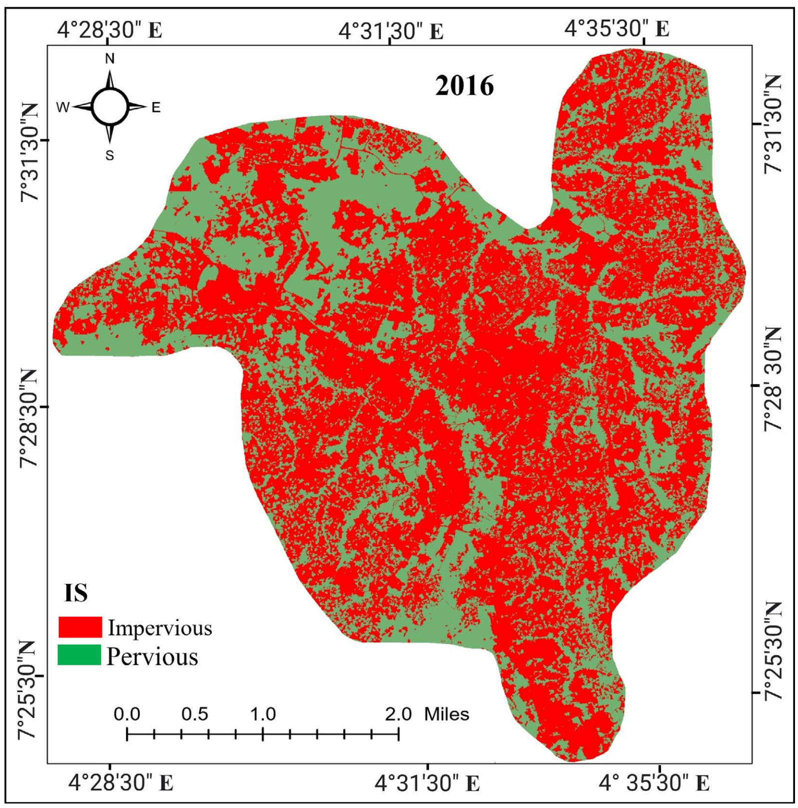

(B)

Figure 4. Reclassified object-based images for 2008 and 2016.

2008 and 2016. When the 2008 land use land cover classification is compared with the 2016 LULC classification, some changes show a reduction or increase in specific LULC. The rate of change in watersheds A, B, C, E, and F amounted to 94.46 ha, 70.24 ha, 511.77 ha, 23.79 ha and 208.08 ha respectively. Vegetation in these watersheds amounted to −93.05 ha, −69.69 ha, −526.68 ha, −24.42 ha and 199.96 ha respectively. The rate of change in another watershed is represented in Table 6.

Accuracy Assessment of the OBIA Classification

Table 7 describes the OBIA classification accuracy assessment carried out. The overall classification accuracy was 87.97% and the overall kappa statistic was 0.81. The producer's accuracy for the combined Built up/water was 77.82%, for

Table 6. Rate of change of land use land cover classification for each watershed.

Watershed	Year	Class names (%)				
		Built up (ha)	Vegetation (ha)	Road (ha)	Water (ha)	Total
A	2008	287.01 (59)	197.82 (41)	0.57 (0)	-	100
	2016	381.47 (78)	104.77 (22)	1.35 (0)	-	100
	Δ	94.46	−93.05	0.78	-	
B	2008	117.45 (52)	104.67 (47)	1.44 (1)	-	100
	2016	189.69 (84)	34.98 (15)	2.61 (1)	-	100
	Δ	70.24	−69.69	1.17	-	
C	2008	1111.41 (50)	1054.89 (47)	30.61 (1)	47.75 (2)	100
	2016	1623.18 (73)	528.21 (24)	37.53 (2)	36.72 (1)	100
	Δ	511.77	−526.68	6.92	−11.03	
D	2008	950.31 (63)	535.41 (36)	16.68 (1)	-	100
	2016	908.23 (60)	579.46 (39)	17.19 (1)	-	100
	Δ	−42.08	44.05	0.51	-	
E	2008	85.68 (60)	56.97 (40)	–	-	100
	2016	109.47 (78)	32.55 (22)	–	-	100
	Δ	23.79	−24.42	–	-	
F	2008	629.82 (58)	452.61 (41)	5.0 (1)	-	100
	2016	834.90 (76)	252.65 (23)	5.5 (1)	-	100
	Δ	208.08	−199.96	0.5	-	
G	2008	1322.64 (66)	674.28 (34)	7.84 (1)	-	100
	2016	1289.94 (64)	713.985 (35)	11.25 (1)	-	100
	Δ	−32.7	39.705	3.41	-	
TOTAL	2008	4504.32	3076.65	62.74	47.75	7691.5
	2016	5324.91	2246.6	73.26	36.72	7691.5

Table 7. Accuracy assessment result of the OBIA classification.

Classified	Built up/Road	Vegetation	Water	User's Accuracy	Kappa
Built up/Road	32	5	0	94.86%	0.92
Vegetation	12	21	0	81.72%	0.75
Water	0	1	14	96.24%	0.94
Producer Accuracy	77.82%	91.56%	100.00%		
Overall Accuracy	87.97%				
Overall Kappa Statistics	0.81				

vegetation was 91.56%, and water was 100%. The user's accuracy for the combined Built up/water was 94.86%, for vegetation it was 81.72%, and for the water class, it was 96.24%. The kappa by landcover class was 0.92 for combined Built up/water, 0.75 for vegetation, and 0.94 for water class. The vegetation landcover class with a user's accuracy of 81.72% and the impervious landcover class with a producer's accuracy of 77.82% explained the overall accuracy of 87.97%. The accuracy assessment result assisted in the further breakdown of the different watersheds into different classes.

3.6. Watershed Impervious Classification

Each of the watersheds was reclassified into impervious and pervious layers. Built-up and roads were classified under impervious while vegetation and water were classified under pervious as shown in Figure 5.

3.7. Water Quality Determination on Impervious Surface Analyst Tool (ISAT)

The effect of imperviousness on water quality was determined using the ISAT tool and an ISAT map was generated, this showed the level of impact (Table 8, Figure 6 and Figure 7). The ISAT map was derived through integration and analysis of processes. The result presented the high, medium and low levels of impact in the study area accounted for 25 - 100, 10 - 25 and 0 - 10 respectively. It was observed that the Built up (impervious) areas have a very high level of impact on the water body in that region, the regions of medium impact were areas with less dense impervious surfaces and some surrounding vegetation and the areas of low impact were observed to be at areas with very little or no human activity, areas with much dense vegetation. A water quality field survey was carried out to verify the various regions of impact as generated by the impervious surface analyst tool. A water quality field survey was carried out to verify the various regions of impact as generated by the impervious surface analyst tool. Water samples were collected from two different locations in the low region and water samples were collected at three different locations in both the medium and high regions of impact, as generated by ISAT.

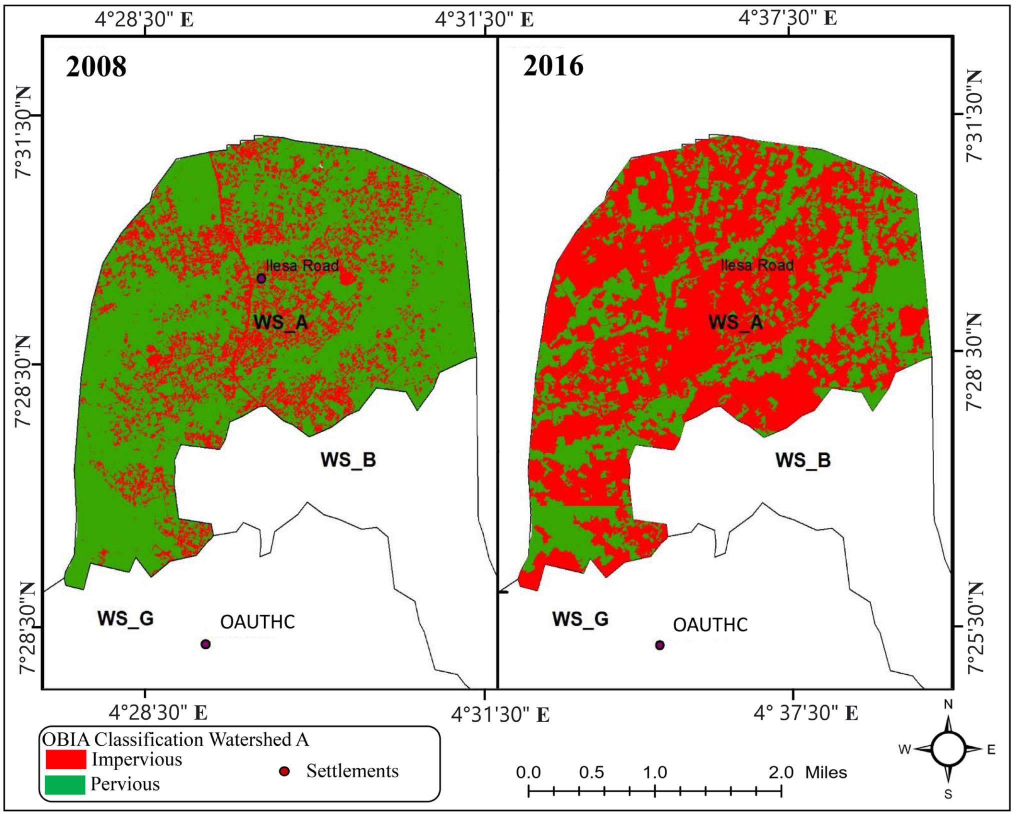
4°28'30" E
4°31'30" E
4°37'30" E
2008
2016
7°31'30"N
7°28'30"N
7°28'30"N
7°31'30"N
7°28' 30"N
7°25'30"N
Ilesa Road
WS_A
WS_B
WS_G
OAUTHC
OBIA Classification Watershed A
Impervious
Pervious
Settlements
0.0 0.5 1.0 2.0 Miles
N
E
S
W

(A)

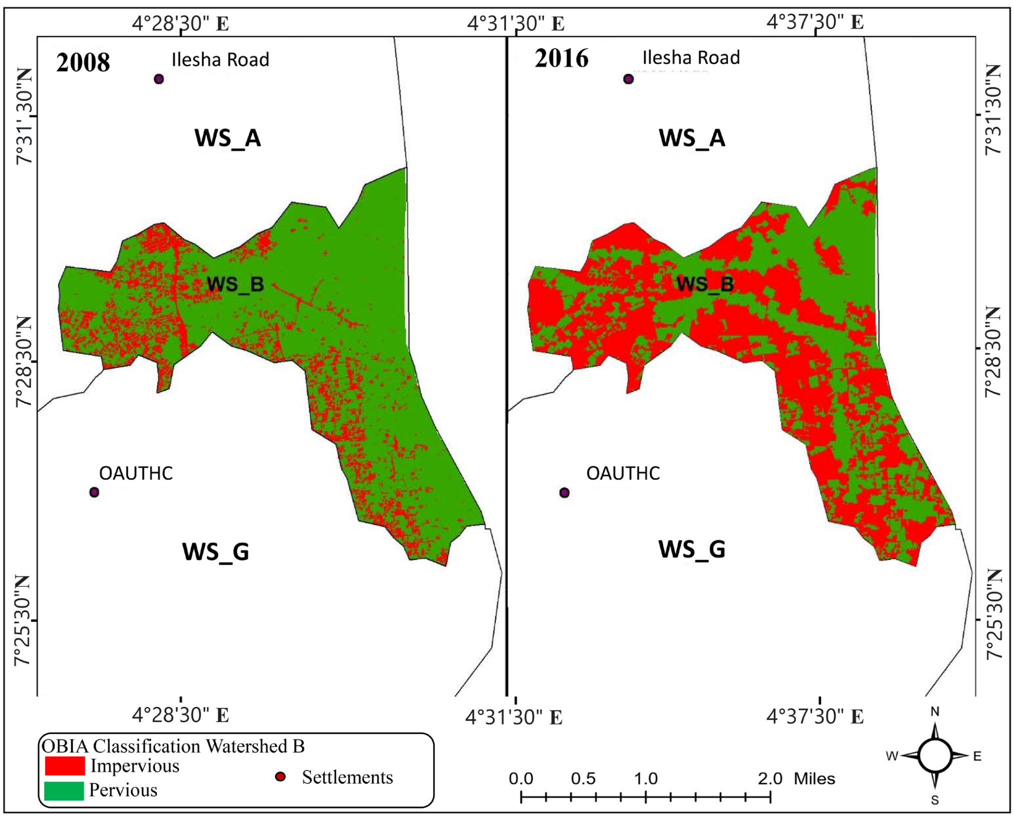
4°28'30" E
4°31'30" E
4°37'30" E
2008
2016
Ilesha Road
WS_A
WS_B
WS_G
OAUTHC
7°31' 30"N
7°28'30"N
7°25'30"N
7°31'30"N
7°28'30"N
7°25'30"N
OBIA Classification Watershed B
Impervious
Pervious
Settlements
0.0 0.5 1.0 2.0 Miles
N
E
S
W

(B)

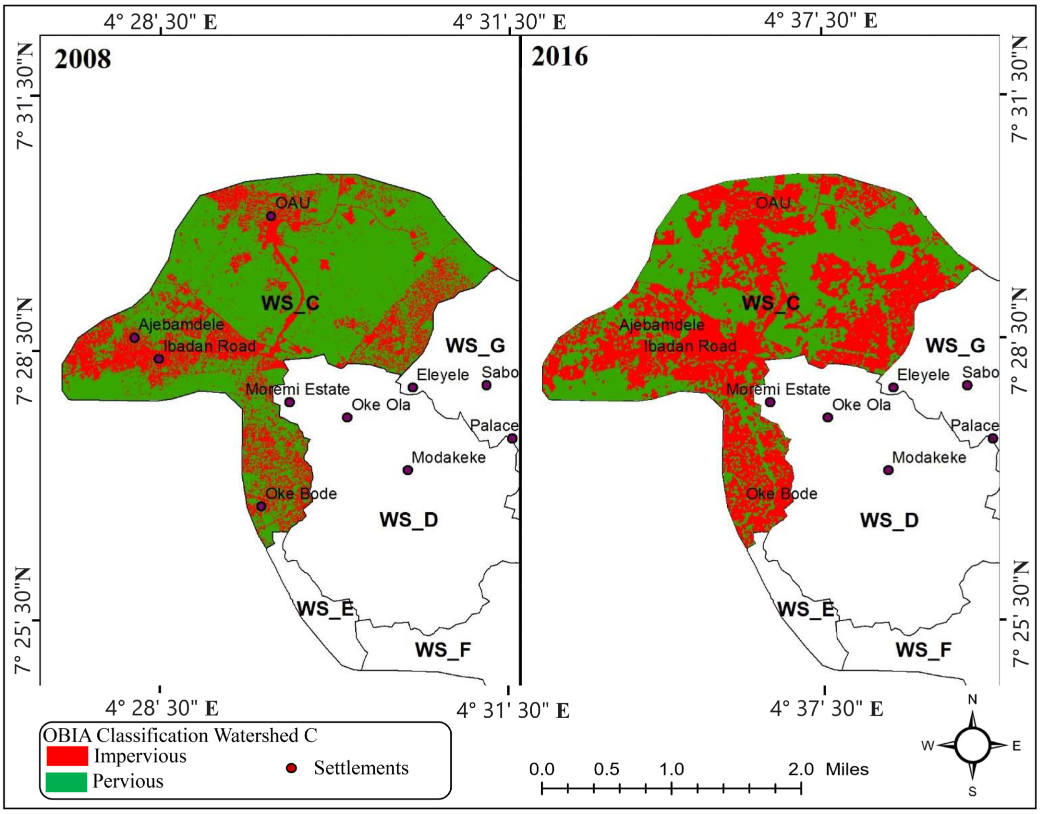
2008
2016
4° 28' 30" E
4° 31' 30" E
4° 37' 30" E
7° 31' 30"N
7° 28' 30"N
7° 25' 30"N
OAU
WS_C
Ajebamdele
Ibadan Road
WS_G
Eleyele
Sabo
Moremi Estate
Oke Ola
Palace
Modakeke
Oke Bode
WS_D
WS_E
WS_F
OBIA Classification Watershed C
Impervious
Pervious
Settlements
0.0 0.5 1.0 2.0 Miles
N
W
E
S

(C)

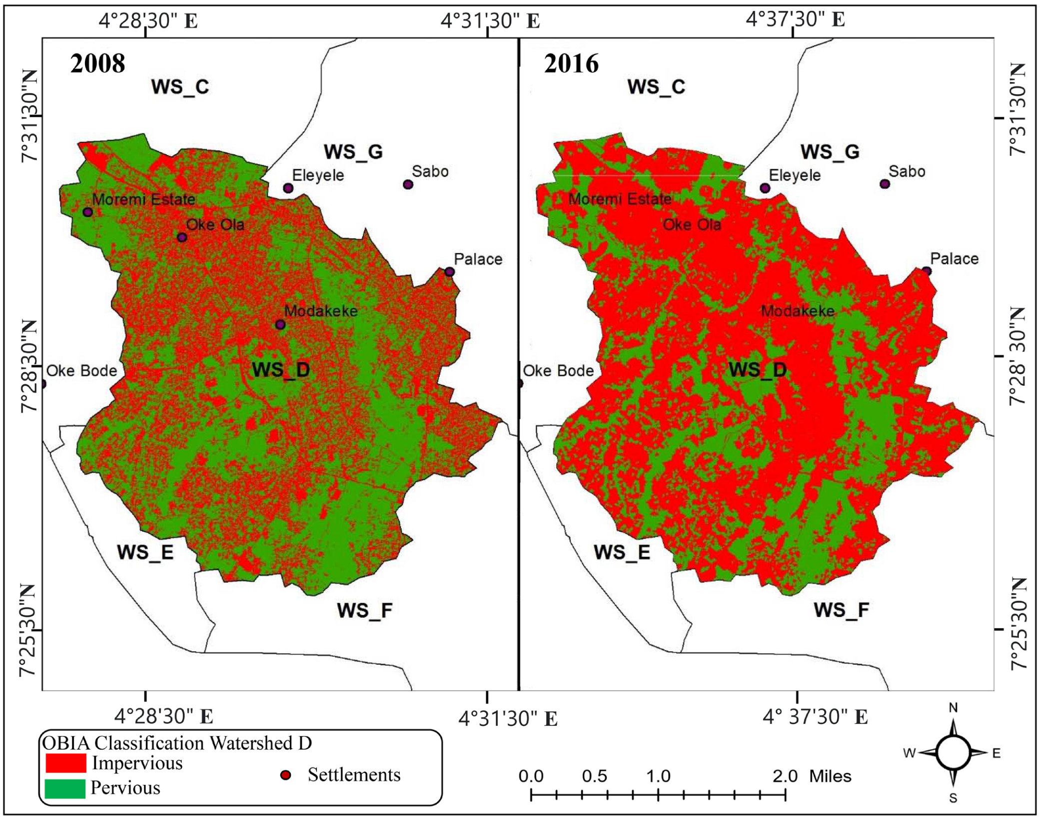
2008
2016
4°28'30" E
4°31'30" E
4°37'30" E
7°31'30"N
7°28'30"N
7°25'30"N
WS_C
WS_G
Eleyele
Sabo
Moremi Estate
Oke Ola
Palace
Modakeke
Oke Bode
WS_D
WS_E
WS_F
OBIA Classification Watershed D
Impervious
Pervious
Settlements
0.0 0.5 1.0 2.0 Miles
N
W
E
S

(D)

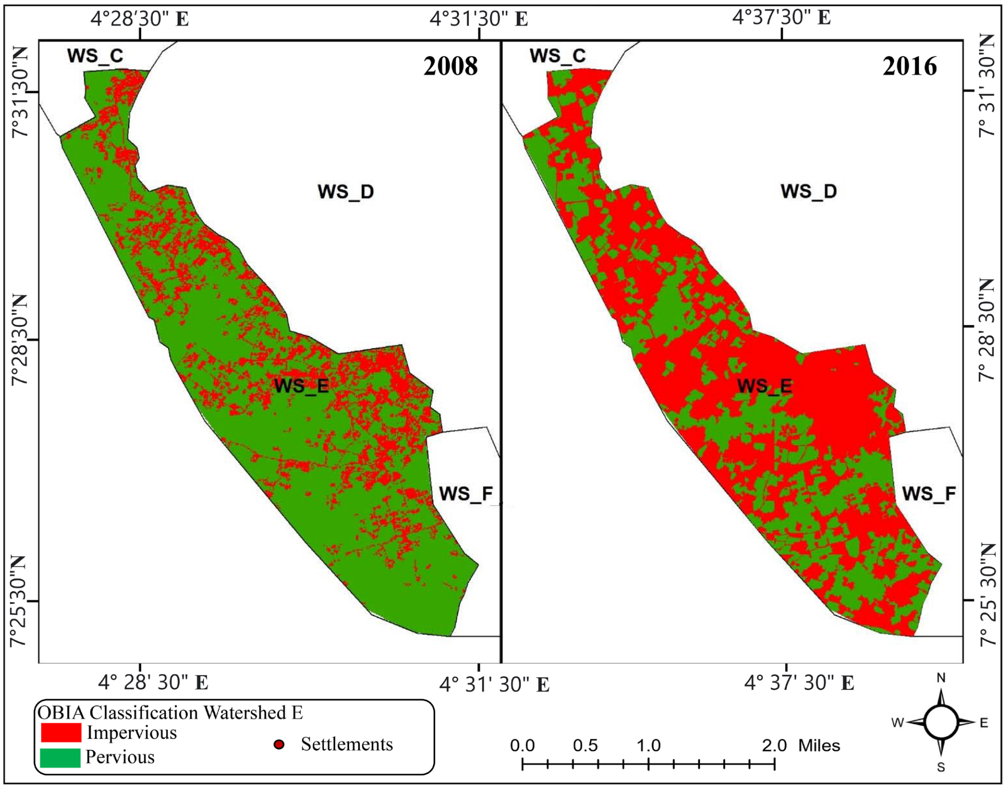

4°28'30" E
4°31'30" E
4°37'30" E
WS_C
2008
2016
WS_D
WS_E
WS_F
7°31'30"N
7°28'30"N
7°25'30"N
4° 28' 30" E
4° 31' 30" E
4° 37' 30" E
OBIA Classification Watershed E
Impervious
Pervious
Settlements
0.0 0.5 1.0 2.0 Miles
N
W
E
S

(E)

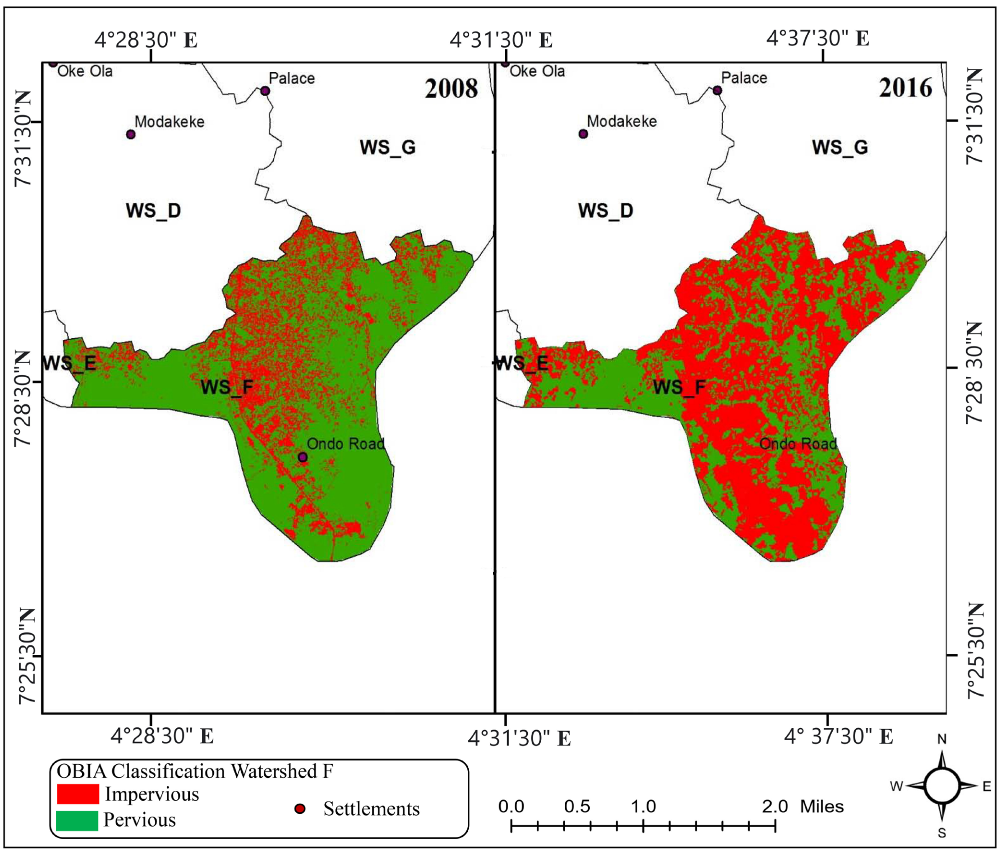

4°28'30" E
4°31'30" E
4°37'30" E
Oke Ola
Palace
Modakeke
2008
2016
WS_G
WS_D
WS_E
WS_F
Ondo Road
7°31'30"N
7°28'30"N
7°25'30"N
4°28'30" E
4°31'30" E
4° 37'30" E
OBIA Classification Watershed F
Impervious
Pervious
Settlements
0.0 0.5 1.0 2.0 Miles
N
W
E
S

(F)

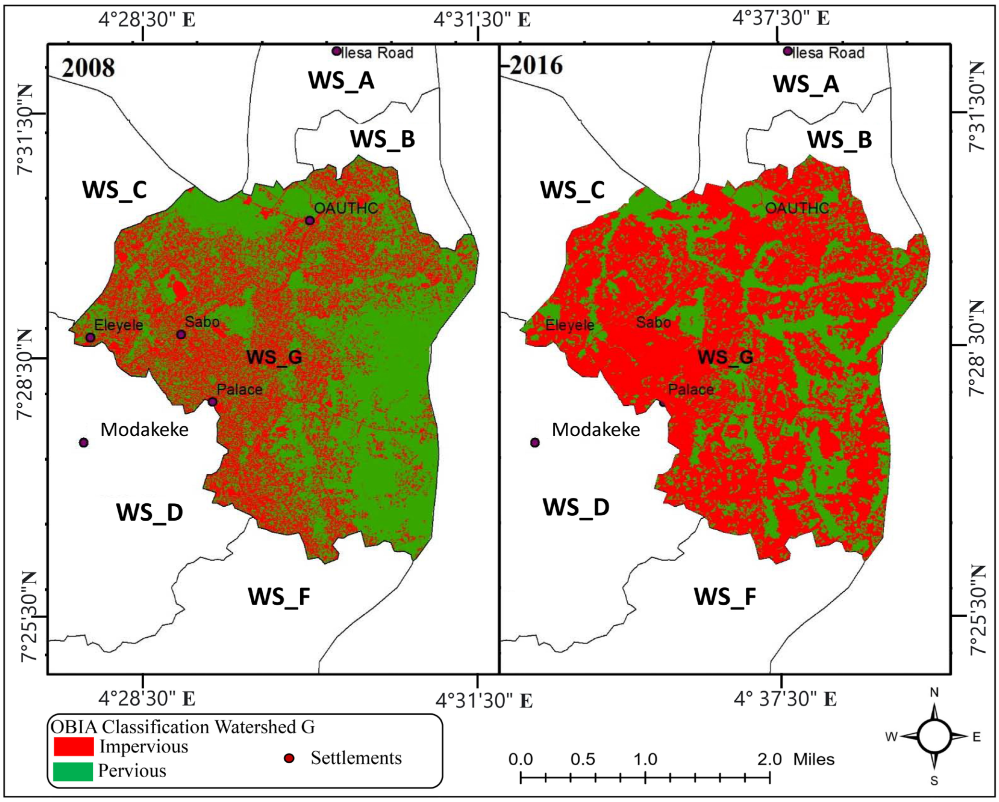

(G)

Figure 5. Reclassified OBIA of each watershed (A-G).

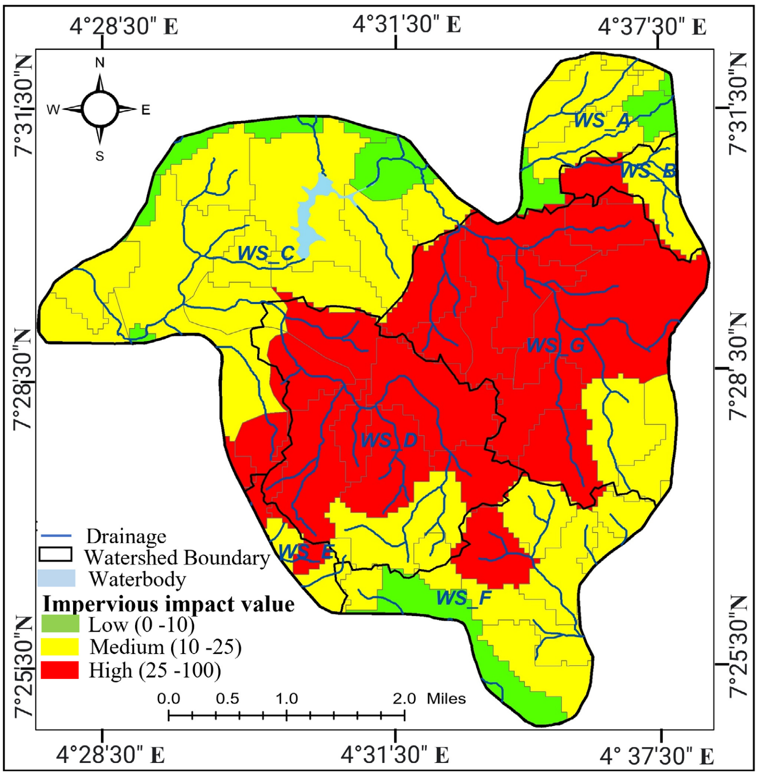

Figure 6. Derived impervious surface of Ile-Ife watershed.

Table 8. Generated level of imperviousness for water quality assessment

Range	Locations	Parameters					
		Temperature (˚C)	TDS (mg/L)	Conductivity (mS/cm)	DO (mg/L)	Turbidity (NTU)	BOD (mg/L)
Low	Central Market	27.9	78	165	4	55.7	0.7
	Hezekiah Oluwasanmi Bridge (Road 7 Bridge)	25.3	93	197	6	32.3	0.5
Medium	Asherifa Foot Bridge	25.2	100	212	7.6	55.9	2.6
	OAUTHC	24.7	145	306	5.6	34.6	3.5
	Maintenance Bridge	25.8	84	178	10	57.5	3.2
High	Ondo Road	25.0	220	463	6.8	82.4	6.8
	Igboya Road Bridge	25.0	341	729	7.2	28.4	1.6
	Aladanla Line 1	25.0	160	246	4	54.8	4.8

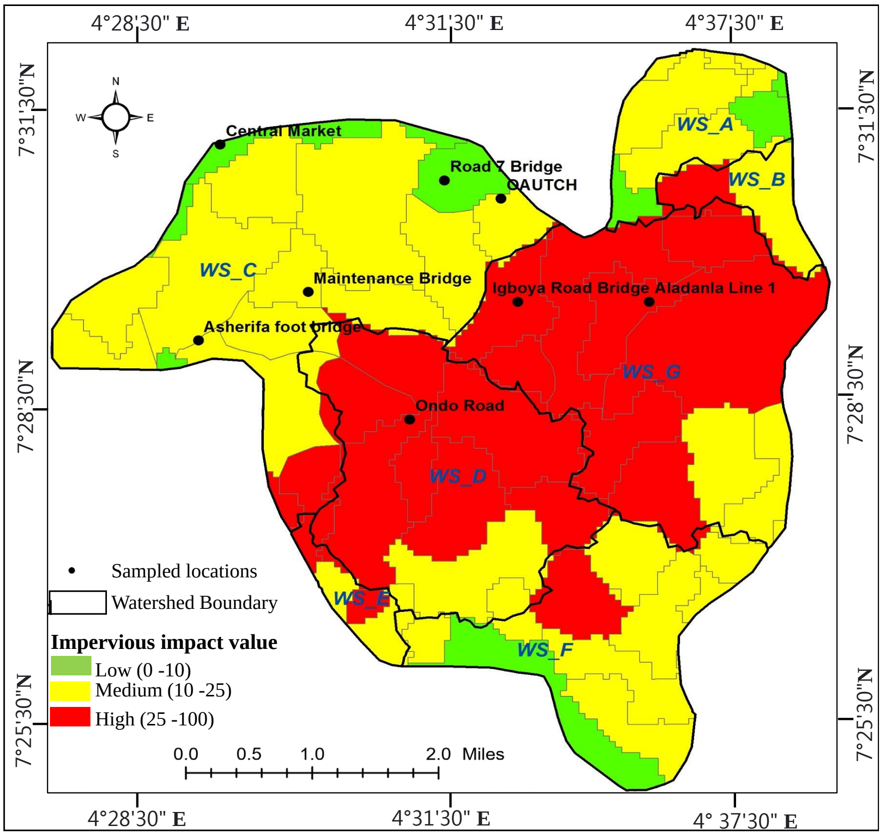

Figure 7. Derived impervious surfaces and assessed water quality locations in Ile-Ife watershed.

4. Discussion and Conclusion

The LULC change documented in the research area affected mainly the conversion of vegetated areas to Built up in the watershed. Population growth applies pressure on land and hence influences land use change altogether, especially to supply new regions for improvement. Vegetation was at its maximum in the year 2008 with 40% of the land cover, then experienced a drastic reduction in the year 2016 to 29%. Furberg and Ban (2012) and Ige-Olumide and Salami (2018) studies agree with the research that the loss of these vegetated regions implies a broader cover by unnatural surfaces and few natural actions given by vegetation, for example, penetration, filtration and assurance against flood and erosion. An increase in impervious covers in the study area could prevent or upset the normal cycles that offer environmental types of services, for example, protection of wide life ecosystem, flood control and guidelines and water quality sustainability, to the district (Salzman et al., 2001). The decrease in vegetation cover has led to increased Built up and thus, impervious, exposing the urban watershed to incessant flooding over the years, including 2010 and 2014 (Liu et al., 2012; Akinwumiju, 2016). Orimoogunje et al. (2016), Rain et al. (2011) and Guyekye (2013) pointed out that decrease in vegetation cover results in increase in impervious surfaces, urban heat islands, and loss of biodiversity and incessant flooding.

The Built up that experienced an increase within the study area is suggestive of an increase in population and infrastructure. As urbanization continues to expand, there is increased pressure on the environment which could lead to environmental crises especially with a lack of proper management and this also agrees with the work carried out by Adetoro and Salami (2018) and Bennett and Saunders (2010). In a similar study, Mengistu and Salami (2007) attributed continued population expansion (Kuddus et al., 2020) as one of the key factors causing spatial growth of Built up and the related pressure on the available land resources and other land use types prompting land use class transition. Several studies have shown that impervious surfaces tend to grow due to urbanization in most parts of the country (Oyinloye & Kufoniyi, 2011; Obiakor et al., 2012; Jesuleye et al., 2013; Mahmoud et al., 2016; Usman et al., 2018; Wang et al., 2018; Wang et al., 2020). Haphazard development can be observed in the study area which is attributed to the uncontrolled increase in impervious surfaces coupled with the absence of well-defined policy implementation for impervious surfaces. Medium-scale enterprises such as shopping complexes, petrol stations and small-scale businesses are causing the study area to be densely urbanized. This increase in urban density takes a toll on the environmental components in the area, this can be seen in the shrinking water body in the study area, amounting to −0.3% (Elmqvist et al., 2016). The non-point source pollution rate related to impervious surface run-off could increase and result in lowering the water quality within the study area (Kim et al., 2016; Adetoro & Salami, 2018).

An increase in impervious surfaces increases runoff to surface water, thereby reducing the quality of the water. The water analysis carried out supports studies by (Osibanjo et al., 2011; Ajibade, 2004) in Ona and Alaro rivers in Ibadan, it agreeing that runoff harms the physical and chemical parameters of surface water. The results from the water sampling showed high turbidity, low dissolved oxygen, and high electrical conductivity in regions with high imperviousness as generated by the ISAT map. High total dissolved solids found in water reduce light infiltration prompting decreased photosynthesis with effects on both phytoplankton and zooplankton populations. Also, a striking water quality characteristic of surface water in urban areas is high turbidity (Adefemi et al., 2007). Turbidity results revealed that the value from most of the sample points in the high, medium and low areas was higher than the 5.0 NTU limit given by WHO (2008) which could be linked to runoff effects due to an increase in impervious covers (Wakawa et al., 2008). This study also revealed the dependence on UAVs and ground-truthing dependence for accuracy assessment carried out.

The study therefore concludes that as built up and other impervious man-made features increase due to rapid urbanization, Ile-Ife city becomes vulnerable to high runoff and thereby causes flooding. This has become a frequent and reoccurring event in Ile-Ife, such as reduced water quality, degraded and destroyed aquatic and terrestrial habitats. Important land use such as water and wetland were also adversely affected in terms of low quality and reduction in size. Based on the assessment of the LULC, the impervious surface development will continue to increase uncontrolled because of the high demand for land development by the various developers. However, it has been discovered that there is a strong connection between ambient temperature and impervious surfaces as both are critical in the study area. Finally, the increase in impervious surfaces if not checked, could affect other land use and cause an environmental disaster. Further research will focus on the use of artificial intelligence for the assessment of other water quality parameters such as the toxicity level of heavy metals in soil and water in fast-developing towns that are changing to urban centers.

Acknowledgements

The Federal Government of Nigeria and Obafemi Awolowo University are appreciated for the grant awarded under the Tertiary Education Trust Fund (TETFUND) Research Projects (RP) Intervention and DIGITAL GLOBE foundation for the Image award to support this research. Space Applications and Environmental Science Laboratory (SPAEL) appreciates the opportunity to utilize other facilities within the laboratory needed for the success of the research.

Conflicts of Interest

The authors declare no conflicts of interest regarding the publication of this paper.

References

Adefemi, O., Asaolu, S., & Olaofe, O. (2007). Assessment of the Physico-Chemical Status of Water Samples from Major Dams in Ekiti State, Nigeria. *Pakistan Journal of Nutrition, 6,* 657-659. https://doi.org/10.3923/pjn.2007.657.659

Aderogba, K. (2012). Qualitative Study of Recent Floods and Sustainable Growth and Development of Cities and Towns in Nigeria. *International Journal of Basic and Applied Sciences, 1,* 200-216.

Adetoro, O., & Salami, A. (2018). Assessment of Land Surface Temperature and LULC changes and the Antecedent Flood Hazard in Ibadan, Nigeria. *Journal of Ecology and Natural Resources, 2,* 1-11. https://doi.org/10.23880/JENR-16000125

Ahn, S., & Kim, S. (2017). Assessment of Integrated Watershed Health Based on the Natural Environment, Hydrology, Water Quality, and Aquatic Ecology. *Hydrology and Earth System Sciences, 21,* 5583-5602. https://doi.org/10.5194/hess-21-5583-2017

Ajibade, L. (2004). Assessment of Water Quality along River Asa, Ilorin, Nigeria. *The Environmentalist, 24,* 11-18. https://doi.org/10.1023/B:ENVR.0000046342.65791.07

Akinwumiju, A. (2016). Morphometric and Land Use Analysis. Implications on Flood Hazards in Ilesa and Osogbo Metropolis, Osun State Nigeria. *Ethiopian Journal of Environmental Studies & Management, 10,* 229-240. https://doi.org/10.4314/ejesm.v10i2.9

Aladejana, O. (2021). Flood Investigation and Adaptation Strategies through Best Management Practices in an Ungauged Basin in Southwest Nigeria. *African Geographical Review, 40,* 141-162. https://doi.org/10.1080/19376812.2020.1782235

Arnold, C., & Gibbons, C. (1996). Impervious Surface Coverage: The Emergence of a Key Environmental Indicator. *Journal of the American Planning Association, 62,* 243-258. https://doi.org/10.1080/01944369608975688

Bennett, A., & Saunders, D. (2010). Habitat Fragmentation and Landscape Change. In N. S. Sodhi, & P. R. Ehrlich (Eds.), *Conservation Biology for All* (pp. 88-106). Oxford Academic. https://doi.org/10.1093/acprof:oso/9780199554232.003.0006

Blaschke, T. (2010). Object Based Image Analysis for Remote Sensing. *ISPRS Journal of Photogrammetry and Remote Sensing, 65,* 2-16. https://doi.org/10.1016/j.isprsjprs.2009.06.004

Blaschke, T., Kelly, M., & Merschdorf, H. (2015). Chapter: 14. Object Based Image Analysis: Evolution, History, State-of-the-Art and Future Vision. In P. S. Thenkabail (Ed.), *Remote Sensing Handbook; Remotely Data Characterization, Classification, and Accuracies* (pp.275-290). Taylor & Francis.

Brabec, E., Schulte, S., & Richards, P. (2002). Impervious Surfaces and Water Quality: A Review of Current Literature and Its Implications for Watershed Planning. *Journal of Planning Literature, 16,* 499-514. https://doi.org/10.1177/088541202400903563

Brun, S., & Band, L. (2000). Simulating Runoff Behavior in an Urbanizing Watershed. *Computers, Environment and Urban Systems, 24,* 5-22. https://doi.org/10.1016/S0198-9715(99)00040-X

Burton, G. A., & Pitt, R. (2002). *Stormwater Effects Handbook: A ToolBox for Watershed Managers, Scientists, and Engineers*. CRC Press, Inc. https://doi.org/10.1201/9781420036244

Cai, C., Li, P., & Jin, H. (2016). Extraction of Urban Impervious Surface Using Two-Season WorldView-2 Images: A Comparison. *Photogrammetric Engineering & Remote Sensing, 82,* 335-349. https://doi.org/10.14358/PERS.82.5.335

Chen, S., Zhang, X., & Peng, L. (2006). Impervious Surface Coverage in Urban Land Use Based on High Resolution Satellite Images. *Resources Science, 28,* 42-46.

Couch, C., Karecha, J., Nuissl, H. et al. (2005). Decline and Sprawl: An Evolving Type of Urban Development—Observed in Liverpool and Leipzig. *European Planning Studies, 13,* 117-136. https://doi.org/10.1080/0965431042000312433

Daramola, A., & Ibem, I. (2010). Urban Environmental Problems in Nigeria: Implications for Sustainable Development. *Journal of Sustainable Development in Africa, 12,* 124-145. https://core.ac.uk/download/pdf/12356053.pdf

Elmqvist, T., Zipperer, W., & Guneralp, B. (2016). Chapter 10. Urbanization, Habitat Loss, Biodiversity Decline: Solution Pathways to Break the Cycle. In K. Seta, W. D. Solecki, & C. A. Griffith (Eds.), *Routledge Handbook of Urbanization and Global Environmental Change* (pp. 139-151). Routledge.

Espriella, M., Lecours, V., Frederick, P. et al. (2020). Quantifying Intertidal Habitat Relative Coverage in a Florida Estuary Using UAS Imagery and GEOBIA. *Remote Sensing, 12,* Article 677. https://doi.org/10.3390/rs12040677

Fabiyi, O. (2006). Urban Land Use Change Analysis of a Traditional City from Remote Sensing Data: The Case of Ibadan Metropolitan Area Nigeria. *Humanity & Social Science Journal, 1,* 42-46.

Fang, J., Piao, S., Field, C. et al. (2003). Increasing Net Primary Production in China from 1982 to 1999. *Frontiers in Ecology and the Environment, 1,* 293-297. https://doi.org/10.1890/1540-9295(2003)001[0294:INPPIC]2.0.CO;2

Farrell, K. (2017). The Rapid Urban Growth Triad: A New Conceptual Framework for Examining the Urban Transition in Developing Countries. *Sustainability, 9,* Article 1407. https://doi.org/10.3390/su9081407

Feng, Q., Liu, J., & Gong, J. (2015). UAV Remote Sensing for Urban Vegetation Mapping Using Random Forest and Texture Analysis. *Remote Sensing, 7,* 1074-1094. https://doi.org/10.3390/rs70101074

Fernández-Götz, M., Wendling, H., & Winger, K. (Eds.) (2014). *Paths to Complexity: Centralisation and Urbanisation in Iron Age Europe*. Oxbow Books. https://doi.org/10.2307/j.ctvh1dt9v

Flanders, D., Hall-Beyer, M., & Pereverzoff, J. (2003). Preliminary Evaluation of eCognition Object-Based Software for Cut Block Delineation and Feature Extraction. *Canadian Journal of Remote Sensing, 29,* 441-452. https://doi.org/10.5589/m03-006

Flinker, P. (2010). *The Need to Reduce Impervious Cover to Prevent Flooding and Protect Water Quality*. AICP Dodson Associates, Ltd.

Fraser, C., Baltsavias, E., & Gruen, A. (2002). Processing of Ikonos Imagery for Submetre 3D Positioning and Building Extraction. *ISPRS Journal of Photogrammetry and Remote Sensing, 56,* 177-194. https://doi.org/10.1016/S0924-2716(02)00045-X

Fu, Y., Liu, K., Shen, Z. et al. (2019). Mapping Impervious Surfaces in Town-Rural Transition Belts Using China's GF-2 Imagery and Object-Based Deep CNNs. *Remote Sensing, 11,* Article 280. https://doi.org/10.3390/rs11030280

Furberg, D., & Ban, Y. (2012). Satellite Monitoring of Urban Sprawl and Assessment of Its Potential Environmental Impact in the Greater Toronto Area between 1985 and 2005. *Environmental Management, 50,* 1068-1088. https://doi.org/10.1007/s00267-012-9944-0

Furniss, M., Staab, B., Hazelhurst, S. et al. (2010). *Water, Climate Change, and Forests: Watershed Stewardship for a Changing Climate* (75 p). Gen. Tech. Rep. PNW-GTR-812, U.S. Department of Agriculture, Forest Service, Pacific Northwest Research Station. https://doi.org/10.2737/PNW-GTR-812

Gaafar, M., Mahmoud, S., Gan, T. et al. (2020). A Practical GIS-Based Hazard Assessment Framework for Water Quality in Stormwater Systems. *Journal of Cleaner Production, 245,* Article ID: 118855. https://doi.org/10.1016/j.jclepro.2019.118855

Garbrecht, J., & Martz, L. (1997). The Assignment of Drainage Direction over Flat Surfaces in Raster Digital Elevation Models. *Journal of Hydrology, 193,* 204-213. https://doi.org/10.1016/S0022-1694(96)03138-1

Giannoni, F., Roth, G., & Rudari, R. (2005). A Procedure for Drainage Network Identification from Geomorphology and Its Application to the Prediction of the Hydrologic Response. *Advances in Water Resources, 28,* 567-581.

https://doi.org/10.1016/j.advwatres.2004.11.013

Gillies, R., Box, J., Symanzik, J. et al. (2003). Effects of Urbanization on the Aquatic Fauna of the Line Creek Watershed, Atlanta—A Satellite Perspective. *Remote Sensing of Environment, 8,* 411-422. https://doi.org/10.1016/S0034-4257(03)00082-8

González, J., Luvall, J., Rickman, D. et al. (2005). Urban Heat Islands Developing in Coastal Tropical Cities. *Eos, Transactions American Geophysical Union Eos, Transactions American Geophysical Union, 86,* 397-403. https://doi.org/10.1029/2005EO420001

Guyekye, A. (2013). Environmental Change and Flooding in Accra, Ghana. *Sacha Journal of Environmental Studies, 3,* 65-80.

Hassan, A., & Lee, H. (2015). The Paradox of the Sustainable City: Definitions and Examples. *Environment, Development and Sustainability, 17,* 1267-1285. https://doi.org/10.1007/s10668-014-9604-z

Henrys, P., & Jarvis, S. (2019). Integration of Ground Survey and Remote Sensing Derived Data: Producing Robust Indicators of Habitat Extent and Condition. *Ecology and Evolution, 9,* 8104-8112. https://doi.org/10.1002/ece3.5376

Hu, X., & Weng, Q. (2011). Impervious Surface Area Extraction from IKONOS Imagery Using an Object-Based Fuzzy Method. *Geocarto International, 26,* 3-20. https://doi.org/10.1080/10106049.2010.535616

Hua, L., Zhang, X., Nie, Q. et al. (2020). The Impacts of the Expansion of Urban Impervious Surfaces on Urban Heat Islands in a Coastal City in China. *Sustainability, 12,* Article 475. https://doi.org/10.3390/su12020475

Ige-Olumide, O., & Salami, A. (2018). Implication of Land Use Change on Flood Vulnerability in an Urban Watershed of Ibadan. *Journal of Geography, Environment and Earth Science International, 14,* 1-17. https://doi.org/10.9734/JGEESI/2018/36574

Ikokou, G., & Smit, J. (2013). A Technique for Optimal Selection of Segmentation Scale Parameters for Object-oriented Classification of Urban Scenes. *South Africa Journal of Geomatics, 2,* 358-369.

ISO (2016). *International Standard ISO 7027-1:2016(E): Water Quality—Determination of turbidity. Part 1: Quantitative Methods*. International Organization for Standardization.

Jacobson, C. (2011). Identification and Quantification of the Hydrological Impacts of Imperviousness in Urban Catchments: A Review. *Journal of Environmental Management, 92,* 1438-1448. https://doi.org/10.1016/j.jenvman.2011.01.018

Jago-on, K., Kaneko, S., Fujikura, R. et al. (2009). Urbanization and Subsurface Environmental Issues: An Attempt at DPSIR Model Application in Asian Cities. *Science of the Total Environment, 407,* 3089-3104. https://doi.org/10.1016/j.scitotenv.2008.08.004

Jennings, D. B., & Jarnagin, S. T. (2002). Changes in Anthropogenic Impervious Surfaces, Precipitation and Daily Streamflow Discharge: A Historical Perspective in a Mid-Atlantic Subwatershed. *Landscape Ecology, 17,* 471-489. https://doi.org/10.1023/A:1021211114125

Jensen, J., & Cowen, D. (1999). Remote Sensing of Urban/Suburban Infrastructure and Socioeconomic Attributes. *Photogrammetric Engineering and Remote Sensing, 65,* 611-622.

Jenson, S., & Domingue, J. (1998). Extracting Topographic Structure from Digital Elevation Data for Geographic Information System Analysis. *Photogrammetric Engineering and Remote Sensing, 54,* 1593-1600.

Jesuleye, I., Adzandeh, E., & Eguaroje, E. (2013). Geospatial Assessment and Monitoring of the Dynamics of Urban Expansion of Ogbomoso, South-Western Nigeria. *Research*

Journal of Environmental and Earth Sciences, 5, 720-727. https://doi.org/10.19026/rjees.5.5728

Ji, M., & Jensen, J. (1999). Effectiveness of Subpixel Analysis in Detecting and Quantifying Urban Imperviousness from Landsat Thematic Mapper Imagery. *Geocarto International, 14,* 31-39. https://doi.org/10.1080/10106049908542126

Jin, H., Stehman, S. V., & Mountrakis, G. (2014). Assessing the Impact of Training Sample Selection on Accuracy of an Urban Classification: A Case Study in Denver, Colorado. *International Journal of Remote Sensing, 35,* 2067-2081. https://doi.org/10.1080/01431161.2014.885152

Johnson, B., & Xie, Z. (2011). Unsupervised Image Segmentation Evaluation and Refinement Using a Multi-Scale Approach. *ISPRS Journal of Photogrammetry and Remote Sensing, 66,* 473-483. https://doi.org/10.1016/j.isprsjprs.2011.02.006

Kalantar, B., Mansor, S., Sameen, M. et al. (2017). Drone-Based Land-Cover Mapping Using a Fuzzy Unordered Rule Induction Algorithm Integrated into Object-Based Image Analysis. *International Journal of Remote Sensing, 38,* 2535-2556. https://doi.org/10.1080/01431161.2016.1277043

Kauffman, G., & Brant, T. (2000). The Role of Impervious Cover as a Watershed-Based Zoning Tool to Protect Water Quality in the Christina River Basin of Delaware, Pennsylvania, and Maryland. In *Proceedings of the Water Environment Federation, Watershed Management 2000 Conference* (pp. 1-11). Water Environment Federation.

Kaufmann, R., Seto, K., Schneider, A., Liu, Z., Zhou, L. et al. (2007). Climate Response to Rapid Urban Growth: Evidence of a Human-Induced Precipitation Deficit. *Journal of Climate, 20,* 2299-2306. https://doi.org/10.1175/JCLI4109.1

Kim, H., Jeong, H., Jeon, J. et al. (2016). The Impact of Impervious Surface on Water Quality and Its Threshold in Korea. *Water, 8,* Article 111. https://doi.org/10.3390/w8040111

Kuddus, M., Tynan, E., & McBryde, E. (2020). Urbanization: A Problem for the Rich and the Poor? *Public Health Reviews, 41,* Article No. 1. https://doi.org/10.1186/s40985-019-0116-0

Lemenkova, P. (2015). Topology, Homogeneity and Scale Factors for Object Detection: Application of eCognition Software for Urban Mapping Using Multispectral Satellite Image. In *Internet and Society* (pp. 80-85).

Levinson, D. (1998). *Ethnic Groups Worldwide: A Ready Reference Handbook.* Oryx Press.

Li, P., Jiang, L., & Feng, Z. (2013). Cross-Comparison of Vegetation Indices Derived from Landsat-7 Enhanced Thematic Mapper plus (ETM+) and Landsat-8 Operational Land Imager (OLI) Sensors. *Remote Sensing, 6,* 310-329. https://doi.org/10.3390/rs6010310

Li, W., Ouyang, Z., Zhou, W., & Chen, Q. (2011). Effects of Spatial Resolution of Remotely Sensed Data on Estimating Urban Impervious Surfaces. *Journal of Environmental Sciences, 23,* 1375-1383. https://doi.org/10.1016/S1001-0742(10)60541-4

Lindsay, J., Rothwell, J., & Davies, H. (2008). Mapping Outlet Points Used for Watershed Delineation onto DEM Derived Stream Networks. *Water Resource Research, 44,* W08442. https://doi.org/10.1029/2007WR006507

Liu, Y., Wei, Y., Tao, S. et al. (2020). Object-Oriented Detection of Building Shadow in TripleSat-2 Remote Sensing Imagery. *Journal of Applied Remote Sensing, 14,* Article ID: 036508. https://doi.org/10.1117/1.JRS.14.036508

Liu, Z., He, C., Zhang, Q. et al. (2012). Extracting the Dynamics of Urban Expansion in China Using DMSP-OLS Nighttime Light Data from 1992 to 2008. *Landscape and Urban Planning, 106,* 62-72. https://doi.org/10.1016/j.landurbplan.2012.02.013

Lohani, V., Kibler, D., & Chanat, J. (2002). Constructing a Problem-Solving Environment Tool for Hydrologic Assessment of Land Use Change. *Journal of the American Water Resources Association, 38,* 439-452. https://doi.org/10.1111/j.1752-1688.2002.tb04328.x

Lu, D., & Weng, Q. (2004). Spectral Mixture Analysis of the Urban Landscape in Indianapolis with Landsat ETM+ Imagery. *Photogrammetric Engineering and Remote Sensing, 70,* 1053-1062. https://doi.org/10.14358/PERS.70.9.1053

Lu, D., & Weng, Q. (2006). Use of Impervious Surface in Urban Land Use Classification. *Remote Sensing of Environment, 102,* 146-160. https://doi.org/10.1016/j.rse.2006.02.010

Lu, D., & Weng, Q. (2009). Extraction of Urban Impervious Surfaces from IKONOS Imagery. *International Journal of Remote Sensing, 30,* 1297-1311. https://doi.org/10.1080/01431160802508985

Lu, D., Moran, E., Hetrick, S. et al. (2011). Land-Use and Land-Cover Change Detection. In Q. Weng (Ed.), *Advances in Environmental Remote Sensing Sensors, Algorithms, and Applications* (pp. 273-290). CRC Press, Taylor & Francis Group. https://doi.org/10.1201/b10599-18

Luo, L., & Mountrakis, G. (2010). Integrating Intermediate Inputs from Partially Classified Images within a Hybrid Classification Framework: An Impervious Surface Estimation Example. *Remote Sensing of Environment, 114,* 1220-1229. https://doi.org/10.1016/j.rse.2010.01.008

Luo, Y., Su, B., Yuan, J. et al. (2011). IS Techniques for Watershed Delineation of SWAT Model in Plain Polders. *Procedia Environmental Sciences, 10,* 2050-2057. https://doi.org/10.1016/j.proenv.2011.09.321

Mabogunje, A. (1968). *Urbanization in Nigeria*. London University Press.

Mabogunje, A. (1980). *The Development Process. A Spatial Perspective*. Unwin Hayman Limited.

Mahmoud, M., Duker, A., Conrad, C. et al. (2016). Analysis of Settlement Expansion and Urban Growth Modelling Using Geoinformation for Assessing Potential Impacts of Urbanization on Climate in Abuja City, Nigeria. *Remote Sensing, 8,* Article 220. https://doi.org/10.3390/rs8030220

Makinde, O., Salami, A., Olaleye, J. et al. (2016). Object Based and Pixel Based Classification Using Rapideye Satellite Imager of ETI-OSA, Lagos, Nigeria. *Geoinformatics FCE CTU, 15,* 59-69. https://doi.org/10.14311/gi.15.2.5

Mengistu, D., & Salami, A. (2007). Application of Remote Sensing and GIS in Land Use Land Cover mapping and Change Detection in a Part of South Western Nigeria. *African Journal of Environmental Science and Technology, 1,* 99-109.

Millennium Ecosystem Assessment (MEA) (2005). *A Report of the Millennium Ecosystem Assessment. Ecosystems and Human Well-Being*. Island Press.

Montgomery, M. (2008). The Urban Transformation of the Developing World. *Science, 319,* 761-764. https://doi.org/10.1126/science.1153012

Morabito, M., Crisci, A., Georgiadis, T., Orlandini, S. et al. (2018). Urban Imperviousness Effects on Summer Surface Temperatures nearby Residential Buildings in Different Urban Zones of Parma. *Remote Sensing, 10,* Article 26. https://doi.org/10.3390/rs10010026

Mugiraneza, T., Ban, Y., & Haas, J. (2019a). Urban Land Cover Dynamics and Their Impact on Ecosystem Services in Kigali, Rwanda Using Multi-Temporal Landsat Data. *Remote Sensing Applications: Society and Environment, 13,* 234-246. https://doi.org/10.1016/j.rsase.2018.11.001

Mugiraneza, T., Nascetti, A., & Ban, Y. (2019b). WorldView-2 Data for Hierarchical Object-Based Urban Land Cover Classification in Kigali: Integrating Rule-Based Approach with Urban Density and Greenness Indices. *Remote Sensing, 11,* Article 2128. https://doi.org/10.3390/rs11182128

National Population Commission (NPC) [Nigeria] (2015). *Nigeria Demographic and Health Survey 2018.*

Nouri, H., Beecham, S., Anderson, S. et al. (2014). High Spatial Resolution WorldView-2 Imagery for Mapping NDVI and Its Relationship to Temporal Urban Landscape Evapotranspiration Factors. *Remote Sensing, 6,* 580-602. https://doi.org/10.3390/rs6010580

O'Callaghan, J., & Mark, D. (1984). The Extraction of Drainage Networks from Digital Elevation Data. *Computer Vision, Graphics and Image Processing, 28,* 328-344. https://doi.org/10.1016/S0734-189X(84)80011-0

Obiakor, M., Ezeonyejiaku, C., & Mogbo, T. (2012). Effect of Vegetated and Synthetic (Impervious) Surfaces on the Microclimate of Urban Area. *Journal of Applied Sciences and Environmental Management, 16,* 85-94.

Olupona, J. (2011). *City of 201 Gods: Ile-Ife in Time, Space and Imagination.* University of California Press. https://doi.org/10.1525/9780520948549

Orimoogunje, O., Fashae, O., Oke, T. et al. (2016). Flood Vulnerability in a Part of Southwestern Nigeria. *Academic Journal of Environmental Science, 4,* 55-61.

Osibanjo, O., Daso, A., & Gbadebo, A. (2011). The Impact of Industries on Surface Water Quality of River Ona and River Alaro in Oluyole Industrial Estate, Ibadan, Nigeria. *African Journal of Biotechnology, 10,* 696-702.

Oyinloye, M., & Kufoniyi, O. (2011). Analysis of Land-Use/Land-COVER and Urban Expansion in Akure. *Journal of Innovative Research in Engineering and Sciences, 2,* 234-248.

Parece, T., & Campbell, J. (2013). Comparing Urban Impervious Surface Identification Using Landsat and High-Resolution Aerial Photography. *Remote Sensing, 5,* 4942-4960. https://doi.org/10.3390/rs5104942

Park, H., Kim, N., Park, S. et al. (2020). Sharpening of Worldview-3 Satellite Images by Generating Optimal High-Spatial-Resolution Images. *Applied Sciences, 10,* Article 7313. https://doi.org/10.3390/app10207313

Paul, M., & Meyer, J. (2001). Streams in the Urban Landscape. *Annual Review of Ecological Systems, 32,* 333-365. https://doi.org/10.1146/annurev.ecolsys.32.081501.114040

Popoola, O., Salami, A., & Adepoju, K. (2016). Assessment and Inventory of Palms in a Plantation by Template Matching of Unmanned Aerial Vehicle (UAV) Image. *Journal of Scientific Research and Reports, 2,* 1-8. https://doi.org/10.9734/JSRR/2016/26948

Powell, R., Roberts, D., Dennison, P. et al. (2007). Sub-Pixel Mapping of Urban Land Cover Using Multiple Endmember Spectral Mixture Analysis: Manaus, Brazil. *Remote Sensing of Environment, 106,* 253-267. https://doi.org/10.1016/j.rse.2006.09.005

Pu, R., Kelly, M., Anderson, G. et al. (2008). Using CASI Hyperspectral Imagery to Detect Mortality and Vegetation Stress Associated with a New Hardwood Forest Disease. *Photogrammetric Engineering and Remote Sensing, 74,* 65-75. https://doi.org/10.14358/PERS.74.1.65

Raddad, S., Salleh, A. et al. (2010). Determinants of Agriculture Land Use Change in Palestinian Urban Environment: Urban Planners at Local Governments Perspective. *American-Eurasian Journal of Sustainable Agriculture, 4,* 30-38.

Rahman, A., Kumar, Y., Fazal, S. et al. (2011). Urbanization and Quality of Urban Environment Using Remote Sensing and GIS Techniques in East Delhi-India. *Journal of*

Geographic Information System, 3, 62-84. https://doi.org/10.4236/jgis.2011.31005

Rain, D., Engstrom, R., Ludlow, C. et al. (2011). *Accra Ghana: A City Vulnerable to Flooding and Drought-Induced Migration* (pp. 3-9). Global Report on Human Settlements.

Rana, M. (2011). Urbanization and Sustainability: Challenges and Strategies for Sustainable Urban Development in Bangladesh. *Environment, Development and Sustainability, 13,* 237-256. https://doi.org/10.1007/s10668-010-9258-4

Raudsepp-Hearne, C., Peterson, G., Tengö, M. et al (2011). The Paradox Persists: How to Resolve It? *BioScience, 61,* 11-12. https://doi.org/10.1525/bio.2011.61.1.4

Ritchie, H., & Roser, M. (2018). *Urbanization*. https://ourworldindata.org/urbanization

Russakovsky, O., Deng, J., Su, H. et al. (2015). ImageNet Large Scale Visual Recognition Challenge. *International Journal of Computer Vision, 115,* 211-252. https://doi.org/10.1007/s11263-015-0816-y

Salzman, J., Thompson Jr., B., & Daily, G. (2001). Protecting Ecosystem Services: Science, Economics, and Law. *Standard Environmental Law Journal, 20,* 300-309.

Shao, M., Tang, X., Zhang, Y. et al. (2006). Environmental Pollution of City Clusters in China: Current Situation and Challenges. *Frontiers in Ecology and the Environment, 4,* 353-361. https://doi.org/10.1890/1540-9295(2006)004[0353:CCICAA]2.0.CO;2

Sugg, Z. et al. (2014). Mapping Impervious Surfaces Using Object-Oriented Classification in a Semiarid Urban Region. *Photogrammetric Engineering & Remote Sensing, 80,* 343-352. https://doi.org/10.14358/PERS.80.4.343

Sun, C., Chen, H., & Fan, F. (2020). Improving Accuracy of Impervious Surface Extraction Based on a Threshold Hierarchical Method (THM). *Applied Sciences, 10,* Article 1. https://doi.org/10.3390/app10010001

Tarboton, D. (1997). A New Method for the Determination of Flow Directions and Contributing Areas in Grid Digital Elevation Models. *Water Resources Research, 33,* 309-319. https://doi.org/10.1029/96WR03137

United Nations (2013). *Population, Development and the Environment 2013*. http://www.un.org/en/development/desa/population/publications/pdf/development/pde_wallchart_2013.pdf

United States Environmental Protection Agency (USEPA) (2003). *LT1ESTWR Disinfection Profiling and Benchmarking Technical Guidance Manual*. Office of Water, US Environmental Protection Agency.

Usman, V., Makinde, O., & Salami, A. (2018). Geospatial Assessment of the Impact of Urban Sprawl in Akure, Southwestern Nigeria. *Journal of Geoscience and Environmental Protection, 6,* 123-140. https://doi.org/10.4236/gep.2018.64008

Wakawa, R., Uzairu, A., Kagbu, J. et al. (2008). Impact Assessment of Effluent Discharge on Physico-Chemical Parameters and Some Heavy Metal Concentrations in Surface Water of River Challawa Kano, Nigeria. *African Journal of Pure and Applied Chemistry, 2,* 100-106.

Wang, J., Li, L. et al. (2011). Stream Guiding Algorithm for Deriving Flow Direction from DEM and Location of Main Streams. In *Cold Region Hydrology in a Changing Climate (Proceedings of Symposium H02 Held during IUGG2011 in Melbourne, Australia, July 2011) (IAHS Publ. 346, 2011)* (pp. 198-205).

Wang, L., Xiao, Y., Rao, E. et al. (2018). An Assessment of the Impact of Urbanization on Soil Erosion in Inner Mongolia. *International Journal of Environmental Research and Public Health, 15,* Article 550. https://doi.org/10.3390/ijerph15030550

Wang, W., Wu, T., Li, Y. et al. (2020). Urbanization Impacts on Natural Habitat and

Ecosystem Services in the Guangdong-Hong Kong-Macao "Megacity". *Sustainability, 12,* 66-75. https://doi.org/10.3390/su12166675

Wei, C., & Blaschke, T. (2018). Pixel-Wise vs. Object-Based Impervious Surface Analysis from Remote Sensing: Correlations with Land Surface Temperature and Population Density. *Urban Science, 2,* Article 2. https://doi.org/10.3390/urbansci2010002

Weng, Q., & Lu, D. (2008). A Sub-Pixel Analysis of Urbanization Effect on Land Surface Temperature and Its Interplay with Impervious Surface and Vegetation Coverage in Indianapolis, United States. *International Journal of Applied Earth Observation and Geoinformation, 10,* 68-83. https://doi.org/10.1016/j.jag.2007.05.002

Weng, Q., Lu, D., & Schubring, J. (2004). Estimation of Land Surface Temperature-Vegetation Abundance Relationship for Urban Heat Island Studies. *Remote Sensing of Environment, 89,* 467-483. https://doi.org/10.1016/j.rse.2003.11.005

World Health Organization (WHO) (2008). *Guidelines for Drinking Water Quality [Electronic Resource]: Third Edition, Incorporating the First and Second Addenda, Volume 1, Recommendations* (668 p.). World Health Organization. https://www.who.int/publications/i/item/9789241547611

Wu, C. (2009). Quantifying High-Resolution Impervious Surfaces Using Spectral Mixture Analysis. *International Journal of Remote Sensing, 30,* 2915-2932. https://doi.org/10.1080/01431160802558634

Wu, C., & Murray, A. T. (2003). Estimating Impervious Surface Distribution by Spectral Mixture Analysis. *Remote Sensing of Environment, 84,* 493-505. https://doi.org/10.1016/S0034-4257(02)00136-0

Wu, J. (2013). *Landscape, Hydrological and Social Factors Affecting Water Quantity and Quality in Urban Headwater Streams of Central Iowa*. Graduate Theses, Iowa State University.

Wu, J. (2014). Urban Ecology and Sustainability: The State-of-the-Science and Future Directions. *Landscape and Urban Planning, 125,* 209-221. https://doi.org/10.1016/j.landurbplan.2014.01.018

Xian, G., & Crane, M. (2006). An Analysis of Urban Thermal Characteristics and Associated Land Cover in Tampa Bay and Las Vegas Using Satellite Data. *Remote Sensing of Environment, 104,* 147-156. https://doi.org/10.1016/j.rse.2005.09.023

Xu, H., & Tang, F. (2013). Analysis of New Characteristics of the First Landsat 8 Image and Their Eco-Environmental Significance. *Acta Ecologica Sinica, 33,* 3249-3257. https://doi.org/10.5846/stxb201305030912

Xu, H., Lin, D., & Tang, F. (2012). The Impact of Impervious Surface Development on Land Surface Temperature in a Subtropical City: Xiamen, China. *International Journal of Climatology, 33,* 1873-1883. https://doi.org/10.1002/joc.3554

Yang, L., Huang, C., Homer, C. et al. (2003). An Approach for Mapping Large-Area Impervious Surfaces: Synergistic Use of Landsat-7 ETM+ and High Spatial Resolution Imagery. *Canadian Journal of Remote Sensing, 29,* 230-240. https://doi.org/10.5589/m02-098

Yang, L., Mansaray, L., Huang, J. et al. (2019). Optimal Segmentation Scale Parameter, Feature Subset and Classification Algorithm for Geographic Object-Based Crop Recognition Using Multisource Satellite Imagery. *Remote Sensing, 11,* Article 514. https://doi.org/10.3390/rs11050514

Yao, H., Qin, R., & Chen, X. (2019). Unmanned Aerial Vehicle for Remote Sensing Applications—A Review. *Remote Sensing, 11,* 14-43. https://doi.org/10.3390/rs11121443

Yuan, F. (2008). Land-Cover Change and Environmental Impact Analysis in the Greater

Mankato Area of Minnesota Using Remote Sensing and GIS Modeling. *International Journal of Remote Sensing, 29,* 1169-1184. https://doi.org/10.1080/01431160701294703

Yuan, F., & Bauer, M. (2007). Comparison of Impervious Surface Area and Normalized Difference Vegetation Index as Indicators of Surface Urban Heat Island Effects in Landsat Imagery. *Remote Sensing of Environment, 106,* 375-386. https://doi.org/10.1016/j.rse.2006.09.003

Zhang, B., Zhou, J., Wang, J. N. et al. (2009). Ore Prospecting Using Multi-Information in the Darbut Suture, Xinjiang. *Contributions to Geology and Mineral Resources Research, 24,* 166-171.

Zhang, L. (2012). Economic Migration and Urban Citizenship: The Role of Points Systems. *Population and Development Review, 38,* 503-533. https://doi.org/10.1111/j.1728-4457.2012.00514.x

Zhang, Y., Zhang, H., & Lin, H. (2014). Improving the Impervious Surface Estimation with Combined Use of Optical and SAR Remote Sensing Images. *Remote Sensing of Environment, 141,* 155-167. https://doi.org/10.1016/j.rse.2013.10.028

Zhao, S., Da, L., Tang, Z. et al. (2006). Ecological Consequences of Rapid Urban Expansion: Shanghai, China. *Frontier in Ecology and Environment, 4,* 341-346. https://doi.org/10.1890/1540-9295(2006)004[0341:ECORUE]2.0.CO;2

Zhou, G., Wei, H., & Fu, S. (2019). A Fast and Simple Algorithm for Calculating Flow Accumulation Matrices from Raster Digital Elevation. *Frontiers of Earth Science, 13,* 317-326. https://doi.org/10.1007/s11707-018-0725-9

Zhou, L., Dickinson, R., Tian, Y. et al. (2004). Evidence for a Significant Urbanization Effect on Climate in China. *Proceedings of the National Academy of Sciences of the United States of America, 101,* 9540-9544. https://doi.org/10.1073/pnas.0400357101

Zhou, W., & Troy, A. (2008). An Object-Oriented Approach for Analysing and Characterizing Urban Landscape at the Parcel Level. *International Journal of Remote Sensing, 29,* 3119-3135. https://doi.org/10.1080/01431160701469065